



8-2006

A Hamiltonian-Based Algorithm for Equilibrium Molecular Dynamics Simulation at Constant Chemical Potential

Johanna Marie Reyes

Follow this and additional works at: https://trace.tennessee.edu/utk_gradthes

 Part of the [Chemical Engineering Commons](#)

Recommended Citation

Reyes, Johanna Marie, "A Hamiltonian-Based Algorithm for Equilibrium Molecular Dynamics Simulation at Constant Chemical Potential. " Master's Thesis, University of Tennessee, 2006.
https://trace.tennessee.edu/utk_gradthes/1784

This Thesis is brought to you for free and open access by the Graduate School at TRACE: Tennessee Research and Creative Exchange. It has been accepted for inclusion in Masters Theses by an authorized administrator of TRACE: Tennessee Research and Creative Exchange. For more information, please contact trace@utk.edu.

To the Graduate Council:

I am submitting herewith a thesis written by Johanna Marie Reyes entitled "A Hamiltonian-Based Algorithm for Equilibrium Molecular Dynamics Simulation at Constant Chemical Potential." I have examined the final electronic copy of this thesis for form and content and recommend that it be accepted in partial fulfillment of the requirements for the degree of Master of Science, with a major in Chemical Engineering.

David J. Keffer, Brian J. Edwards, Major Professor

We have read this thesis and recommend its acceptance:

William V. Steele

Accepted for the Council:

Carolyn R. Hodges

Vice Provost and Dean of the Graduate School

(Original signatures are on file with official student records.)

To the Graduate Council:

I am submitting herewith a thesis written by Johanna Marie Reyes Santiago entitled “A Hamiltonian-Based Algorithm for Equilibrium Molecular Dynamics Simulation at Constant Chemical Potential.” I have examined the final electronic copy of this thesis for form and content and recommend that it be accepted in partial fulfillment of the requirements for the degree of Master of Science, with a major in Chemical Engineering.

David J. Keffer

Co-Major Professor

Brian J. Edwards

Co-Major Professor

We have read this thesis and
recommend its acceptance:

William V. Steele

Acceptance for the Council:

Anne Mayhew

Vice Chancellor and
Dean of Graduate Studies

(Original signatures are on file with official student records)

A HAMILTONIAN-BASED ALGORITHM FOR EQUILIBRIUM MOLECULAR
DYNAMICS SIMULATION AT CONSTANT CHEMICAL POTENTIAL

A Thesis
Presented for the
Master of Science Degree
The University of Tennessee, Knoxville

Johanna Marie Reyes Santiago
August 2006

DEDICATION

To my dear family the Santiagos, the Reyeses, the Wests, and the Litchfields
and to my friends Ester, Jun, Gigi, Joy, Gaile, Ronnel, and Lucy

ACKNOWLEDGEMENTS

I would like to thank my academic advisors Dr. David Keffer and Dr. Brian Edwards for their guidance and patience. I also thank Dr. William Steele for sitting in my committee.

I would like to express my appreciation to my lab mates at the Computational Materials Research Group for their encouragement and support.

ABSTRACT

The objective of the research described in this thesis is to determine whether dilating mass can produce an equilibrium molecular dynamics algorithm for rigorous constant chemical potential simulation. The hypothesis is tested by developing an equilibrium molecular dynamics algorithm for the grand ensemble (constant chemical potential, volume and energy ensemble or $\mu V\mathcal{E}$ ensemble) following a methodical procedure developed by Keffer *et al.* [1] and running simulations on possibly a $\mu V\mathcal{E}$ ensemble. A novel concept for a chemicostat controller is described. An equation for the instantaneous chemical potential is not available, thus a property, called the instantaneous partial specific Hamiltonian, that is related to the chemical potential was defined. The Hamiltonian for the $\mu V\mathcal{E}$ ensemble was formulated and from this the equations of motion were derived. The derivation of the algorithm for the integration scheme – single time scale reversible reference system propagator (rRESPA) is presented. We were able to simulate successfully a stable algorithm (*i.e.*, the chemicostat controller functions properly, driving the system to the set point product of the partial specific Hamiltonian and mass), and show an equivalence of the change in mass and the change in number of particles with respect to the change in potential energy. The methodical procedure for algorithm development has great potential for extending the $\mu V\mathcal{E}$ ensemble algorithm to rigorous grand canonical ensemble EMD simulations.

TABLE OF CONTENTS

1	Introduction.....	1
1.1	Background: Motivation for Formulating Constant Chemical Potential Molecular Dynamics Algorithms.....	1
1.2	Synopsis of Chapters.....	2
2	Background Calculations and Derivations.....	3
2.1	Formulating the Hamiltonian for Grand Ensemble Equilibrium Molecular Dynamics	3
2.1.1	The Chemicostat Controller.....	3
2.1.2	Instantaneous Partial Specific Hamiltonian.....	5
2.1.3	$\mu V\mathcal{E}$ Hamiltonian	7
2.2	Derivation of the Equations of Motion	9
2.3	Reversible Reference System Propagator Algorithm (rRESPA) Integration Scheme.....	13
2.3.1	The Liouville Operator	13
2.3.2	The Time Evolution Equations	15
2.3.3	rRESPA Algorithm	18
3	$\mu V\mathcal{E}$ Ensemble Simulations	22
3.1	$\mu V\mathcal{E}$ Ideal Gas	22
3.1.1	Simulation where μ^{*set} is Equal to $\mu^*(t_o)$	24
3.1.2	Simulation where $\mu^{*set} < \mu^*(t_o)$	26
3.2	Dilute Gas Simulations, Forms of the Potential Energy	28
3.2.1	The Specific Potential Energy	28
3.2.2	Potential Energy as a Function of r and ρ	30
3.3	$\mu V\mathcal{E}$ Dilute Gas Simulations Using the Specific Potential Energy.....	33
3.4	$\mu V\mathcal{E}$ Dilute Gas Simulations Using Potential Energy as a Function of r and ρ	34
3.4.1	The Pair Correlation as a Function of r and ρ	34
3.4.2	Simulation Results and Discussions	36
4	Conclusions and Future Work	47
	REFERENCES	49
	APPENDICES	52
	VITA	74

LIST OF TABLES

Table 3.1-1 Simulation Input Parameters for Methane.....	24
Table 3.4-1 Results for Simulations at Different Values of μ^{*set}	38
Table 3.4-2 Results for Simulations at Different Densities	38

LIST OF FIGURES

Figure 3.1-1 Mass vs. simulation steps for an ideal gas system, with $\mu^{*set} = \mu^*(t_o)$	25
Figure 3.1-2 $\mu^*(t)m$ vs. simulation steps for an ideal gas system, with $\mu^{*set} = \mu^*(t_o)$	25
Figure 3.1-3 $\mu^*(t)$ vs. simulation step for an ideal gas system, with $\mu^{*set} = 3.262$	26
Figure 3.1-4 $\mu^*(t)m$ vs. simulation step for an ideal gas system, with $\mu^{*set} = 3.262$	27
Figure 3.1-5 Mass vs. simulation step for an ideal gas system, with $\mu^{*set} = 3.262$	27
Figure 3.3-1 $\mu^*(t)$ vs. simulation step for a dilute gas system, specific potential energy case, with $\mu^{*set} = \mu^*(t_o)$	34
Figure 3.4-1 $\mu^*(t)$ vs. simulation step, from the simulation of a dilute gas system, $U(r,\rho)$ case, with $\mu^{*set} = \mu^*(t_o)$	37
Figure 3.4-2 $\mu^*(t)m$ vs. simulation step from the simulation of a dilute gas system, $U(r,\rho)$ case, with $\mu^{*set} = \mu^*(t_o)$	38
Figure 3.4-3 Mass histogram from the simulation of a dilute gas system, $U(r,\rho)$ case, with $\mu^{*set} = \mu^*(t_o)$	39
Figure 3.4-4 Pair correlation function from the simulation of a dilute gas system, $U(r,\rho)$ case, with $\mu^{*set} = \mu^*(t_o)$	40
Figure 3.4-5 The potential energy from $\mu V\mathcal{E}$, NVE and OZPY vs. density.	43
Figure 3.4-6 The change in potential energy with respect to a change in system density vs. density.	45

1 Introduction

1.1 Background: Motivation for Formulating Constant Chemical Potential Molecular Dynamics Algorithms

There has been extensive research on developing extended-system molecular dynamics (MD) algorithms [1, 2]. Among existing algorithms, there are some that have proven to be rigorous, *i.e.*, these generate trajectories in the corresponding statistical mechanical ensemble. There are notable features in these successful algorithms. Dilating time was essential for the Nosé-Hoover thermostat, which allowed for the rigorous simulation in the canonical (NVT) ensemble under a limited set of constraints [3, 4] and was recently generalized for equilibrium molecular dynamics (EMD) under the imposition of an arbitrary external force [5]. Dilating space was essential for the Nosé barostat, which allowed for the rigorous simulation in the isobaric-isothermal (NpT) and the isobaric-isenthalpic (NpH) ensembles with a limited set of constraints [6]. This has been recently generalized for EMD [7].

The objective of the research described in this thesis is to determine whether dilating mass can produce rigorous MD algorithms for constant chemical potential ensembles. The hypothesis is tested by developing an EMD algorithm and running simulations on a grand ensemble ($\mu V \mathcal{E}$); by grand ensemble we mean constant chemical potential, volume and energy system.

There are existing constant chemical potential MD schemes in the literature [8-10]. These schemes use different techniques, such as a combination of Monte Carlo and MD and allowing for fractional particles, to vary the number of particles in the simulation. The primary difference and advantage of our proposed algorithm is that we would do away with particle insertion and deletion, which has been the common approach to constant chemical potential simulations.

In this research, the correspondence between dilating mass and changing the number of particles in a MD simulation of a $\mu V \mathcal{E}$ ensemble with a constant chemical

potential is evaluated. The result of the constant chemical potential algorithm will be referred to as evolution equations for the chemicostat.

1.2 Synopsis of Chapters

Chapter 2, “Background Calculations and Derivations”, describes the methods used in developing the EMD $\mu V\mathcal{E}$ algorithm. A novel concept for a chemicostat controller is described. An equation for the instantaneous chemical potential is not available, thus we formulate a property, called the instantaneous partial specific Hamiltonian, that is closely related to the chemical potential. The $\mu V\mathcal{E}$ ensemble Hamiltonian is then formulated, from which the equations of motion are derived. In the last section, the integration scheme, a single time scale reversible reference system propagator (rRESPA), for the resulting equations of motion is presented.

Chapter 3, “ $\mu V\mathcal{E}$ Ensemble Simulations”, contains the results of the $\mu V\mathcal{E}$ MD simulations. The algorithm derived in Chapter 2 is applied to an ideal gas system and a dilute gas system. For dilute gas simulations, two different equations for the potential energy are used. In the first equation, potential energy is expressed as the product of the mass of a particle and the specific potential energy. The second equation expresses the potential energy as a function of both particle distance and system density. The second equation resulted in a stable simulation for the dilute gas system and was used to run more simulations to test the algorithm.

Chapter 4 contains conclusions and recommendations for future work.

2 Background Calculations and Derivations

2.1 Formulating the Hamiltonian for Grand Ensemble Equilibrium Molecular Dynamics

2.1.1 The Chemicostat Controller

The controller for the constant chemical potential algorithm is developed analogously to the previous extended-system EMD algorithms, such as the Nosé-Hoover thermostat and the Nosé barostat, as shown below.

In the NVT EMD algorithm, a previously derived evolution equation for the thermostat momentum, ζ_T , is of the form,

$$\frac{d\zeta_T}{dt} = \nu_T^2 \left[\frac{T(t)}{T_{set}} - 1 \right]$$

2-1

where $T(t)$ is the instantaneous temperature, T_{set} is the set point temperature and ν_T is a thermostat controller frequency. From Equation 2-1 we see that there is no change in the thermostat momentum when the system is at the set temperature. Likewise in the NpH EMD algorithm, a previously derived evolution equation for the barostat momentum, $\zeta_{P,\alpha}$, is of the form

$$\frac{d\zeta_{P,\alpha}}{dt} = \frac{1}{\eta_{P,\alpha}^2} \frac{\nu_{P,\alpha}^2 V(t)}{f k_B T} (p_{\alpha\alpha}(t) - p_{set}) - \zeta_{P,\alpha}^2$$

2-2

where $p_{\alpha\alpha}(t)$ is an instantaneous diagonal element of the pressure tensor, p_{set} is the set point pressure, $V(t)$ is the instantaneous volume, f is the number of degrees of freedom, k_B is Boltzmann's constant, $\nu_{P,\alpha}$ is a barostat controller frequency, and $\eta_{P,\alpha}$ is the space dilation variable. Again, we see that there is no change in barostat momentum when the system is at the set pressure. Therefore, when we implement the chemicostat, it is

possible that we will require an evolution equation for the chemicostat momentum, $\zeta_{\mu,\kappa}$, of the form

$$\frac{d\zeta_{\mu,\kappa}}{dt} = f_1(\eta_{\mu,\kappa}, v_{\mu,\kappa}^2)(\mu_{\kappa}(t) - \mu_{set,\kappa}) - f_2(\zeta_{\mu,\kappa})$$

2-3

where $\mu_{\kappa}(t)$ is the instantaneous chemical potential of component κ , $\mu_{set,\kappa}$ is the set point chemical potential of component κ , $v_{\mu,\kappa}$ is a chemicostat controller frequency for component κ , $\eta_{\mu,\kappa}$ is the mass dilation variable for component κ , and f_1 and f_2 are some functions to be determined. However, as shown in Appendix A, we find that this form for the chemicostat controller (equation 2-3) will not function properly. A chemicostat controller of the form,

$$\frac{d\zeta_{\mu,\kappa}}{dt} = f_1(\eta_{\mu,\kappa}, v_{\mu,\kappa}^2)(m\mu_{\kappa}(t) - m'\mu_{set,\kappa}) - f_2(\zeta_{\mu,\kappa})$$

2-4

where m is the dilated particle mass of the particle and m' is the undilated particle mass, will be the focus of interest in this thesis.

In Equations 2-1, 2-2 and 2-4, instantaneous thermodynamic functions for temperature, pressure, and chemical potential were introduced and must be suitably defined. The definition of the instantaneous temperature and the instantaneous pressure come from the “generalized equipartition theorem” [11]. As such, the temperature function is defined as

$$T(t) = \frac{1}{f k_B} \sum_{\alpha=1}^3 \sum_{i=1}^N \frac{p_{i,\alpha}^2}{m_i}$$

2-5

where $p_{i,\alpha}$ is the momentum of particle i in the α dimension, m_i is the mass of a particle i , N is the total number of particles, and f is the number of degrees of freedom. The instantaneous diagonal element of the pressure tensor is defined as

$$p_{\alpha\alpha}(t) = \frac{1}{V(t)} \left[\sum_{i=1}^N \frac{p_{i,\alpha}^2}{m_i} + \sum_{i=1}^N F_{i,\alpha} r_{i,\alpha} \right]$$

2-6

where $r_{i,\alpha}$ and $F_{i,\alpha}$ are the position and force of particle i in the α dimension, respectively. It is obvious that we need an expression for the instantaneous chemical potential in terms of the molecular level properties, including the position, momenta, masses and forces, similar to Equations 2-5 and 2-6. Such an expression does not currently exist.

2.1.2 Instantaneous Partial Specific Hamiltonian

In this section, we derive an expression for the instantaneous partial specific Hamiltonian, a property that is not the same as the traditional chemical potential, but is closely related to it. Therefore, if we have an algorithm for simulations with constant specific partial Hamiltonian, we should have derived an algorithm for simulation in the $\mu V \mathcal{E}$ ensemble.

We now derive an expression for the instantaneous specific partial Hamiltonian of component κ , which will be denoted by the symbol, $\mu_{\kappa}^*(t)$. We start with classical thermodynamics, in which the specific chemical potential of component κ in a multi-component mixture of C components is defined as

$$\mu_{\kappa}(t) \equiv \left(\frac{\partial G}{\partial M_{\kappa}} \right)_{T, p, M_{i \neq \kappa}} = \left(\frac{\partial A}{\partial M_{\kappa}} \right)_{T, V, M_{i \neq \kappa}} = \left(\frac{\partial H}{\partial M_{\kappa}} \right)_{S, p, M_{i \neq \kappa}} = \left(\frac{\partial U}{\partial M_{\kappa}} \right)_{S, V, M_{i \neq \kappa}}$$

2-7

where G is the Gibbs free energy, A is the Helmholtz free energy, H is the enthalpy (distinguished from a Hamiltonian by its lack of subscripts), U is the internal energy, and S is the entropy, all on an extensive basis. Also, M_{κ} is the total mass of component κ , which can be expressed as

$$M_{\kappa} = N_{\kappa} m_{\kappa}$$

2-8

where N_κ is the number of molecules (not atoms) of type κ , and m_κ is the mass of a molecule (not atom) of type κ . We distinguish between molecules and atoms here because classical thermodynamics defines the specific chemical potential on a molecular basis, whereas simulations typically treat particles that correspond to atoms rather than molecules.

In the work of Keffer *et al.* [1] on deriving rigorous EMD algorithms, they observed that the Hamiltonian of a system had a direct relationship to U in NVE, A in NVT, G in NpT, and H in NpH simulations. Therefore, we need only differentiate the Hamiltonian with respect to M_κ in order to obtain an expression that is related to the specific chemical potential. We will refer to this partial derivative as the partial specific Hamiltonian instead of chemical potential because, while related, the two are not equivalent.

Historically, people naturally treated a differentiation with respect to M_κ as equivalent to a differentiation with respect to N_κ , where the mass of a molecule was assumed to be constant, i.e., $dM_\kappa = m_\kappa dN_\kappa$. This is very reasonable thing to do in situations where the mass of a molecule is constant.

In simulations, we have some advantages over the laboratory. We can imagine and implement clever mathematical transformations that are not currently possible in the experimentalist's laboratory. For example, Nosé dilated time and space to develop his thermostat and barostat. Here, we intend to dilate mass, without changing the number of particles in the system. As such, we consider the differentiation of M_κ as equivalent to a differentiation with respect to m_κ , where the number of molecules is assumed to be constant, i.e., $dM_\kappa = N_\kappa dm_\kappa$. Therefore, when we substitute this into equation 2-7, we will have

$$\mu_\kappa^*(t) = \frac{1}{N_\kappa} \left(\frac{\partial H_{NpT}}{\partial m_\kappa} \right)_{T,p,M_{i \neq \kappa}} = \frac{1}{N_\kappa} \left(\frac{\partial H_{NVT}}{\partial m_\kappa} \right)_{T,V,M_{i \neq \kappa}} = \frac{1}{N_\kappa} \left(\frac{\partial H_{NpH}}{\partial m_\kappa} \right)_{S,p,M_{i \neq \kappa}} = \frac{1}{N_\kappa} \left(\frac{\partial H_{NVE}}{\partial m_\kappa} \right)_{S,V,M_{i \neq \kappa}} \quad \mathbf{2-9}$$

In a single-component monatomic system in the microcanonical ensemble, the Hamiltonian can be written as

$$H_{NVE} = \frac{1}{2} \sum_{\alpha=1}^3 \sum_{i=1}^N m v_{i,\alpha}^2 + \sum_{i=1}^N U_i$$

2-10

where N is the number of particles, U_i is the potential energy for particle i ., and $v_{i,\alpha}$ is the velocity of the i^{th} particle in the α dimension. We substitute Equation 2-10 into Equation 2-9 and evaluate the derivative to get the expression for the partial specific Hamiltonian for a single component:

$$\mu^*(t) = \frac{1}{N} \left(\frac{1}{2} \sum_{\alpha=1}^3 \sum_{i=1}^N v_{i,\alpha}^2 + \sum_{i=1}^N \frac{\partial U_i}{\partial m} \right)$$

2-11

At this point, we have derived $\mu^*(t)$ an instantaneous thermodynamic property, which is easily evaluated from a simulation and is needed for a constant chemical potential algorithm.

2.1.3 $\mu V \mathcal{E}$ Hamiltonian

Having derived an instantaneous specific partial Hamiltonian we must now formulate the Hamiltonian of an extended system. Unlike the first step of the procedure in Keffer *et al.* [1], where the Hamiltonian first had to be expressed in terms of the peculiar and center of mass (COM) coordinates in the mathematical (potentially aphysical) frame of reference, the $\mu V \mathcal{E}$ Hamiltonian can be defined in laboratory coordinates in the mathematical frame of reference. Expressing the Hamiltonian in terms of peculiar and COM coordinates had to be done for the thermostat and barostat algorithms since the time and space dimensions were only dilated for the peculiar variables; one is then able to see intuitively where to insert correctly the time and space dilation variables.

We write the $\mu V \mathcal{E}$ Hamiltonian in terms of particle velocities rather than momenta so it will be clear where to insert the mass dilation variable within the Hamiltonian. The mass dilation variable, $\eta_{\mu,\kappa}$ for component κ , is a multiplier for the undiluted mass

variables, *i.e.*, $m_{j,i,\kappa} = \eta_{\mu,\kappa} m'_{j,i,\kappa}$. Thus we write the Hamiltonian of a multicomponent polyatomic system in the $\mu V \mathcal{E}$ ensemble as

$$H'_{\mu V \mathcal{E}} = \sum_{\kappa=1}^c \sum_{i=1}^{M_{\kappa}} \sum_{j=1}^{N_{i,\kappa}} \sum_{\alpha=1}^3 \frac{\eta_{\mu,\kappa}}{2} m'_{j,i,\kappa} v_{\alpha,j,i,\kappa}^2 + \sum_{\kappa=1}^c \sum_{i=1}^{M_{\kappa}} \sum_{j=1}^{N_{i,\kappa}} U_{j,i,\kappa} \\ + \sum_{\kappa=1}^c \frac{1}{2} \frac{p_{\eta,\kappa}^2}{Q_{\eta,\kappa}} - \sum_{\kappa=1}^c \ln(\eta_{\mu,\kappa}) \mu_{\kappa}^{*set} \sum_{i=1}^{M_{\kappa}} \sum_{j=1}^{N_{i,\kappa}} m'_{j,i,\kappa}$$

2-12

where $p_{\eta,\kappa}$ is the momentum of the mass dilation variable for component κ , $Q_{\eta,\kappa}$ is the inertial mass of the mass dilation variable for component κ , and C is the total number of components. We have primed the variables to indicate that they are defined in a frame of reference before we apply a non-canonical transformation. The penultimate summation on the RHS of the Hamiltonian is the kinetic energy of the mass dilation variables. The last summation on the right hand side (RHS) of the Hamiltonian is the potential energy of the mass dilation variables. The kinetic energy of the mass dilation variables has a functional form that is entirely analogous to that of the time and space dilation variables defined by Nosé [3, 12]. The potential energy of the mass dilation variables has a functional form that is simply a Legendre transformation of the Hamiltonian, completely analogous with the procedure used with the space dilation variable by Nosé.

The Legendre transformation defines our free energy, \mathcal{E} , as

$$\mathcal{E} = U - \sum_{\kappa=1}^c M_{\kappa} \mu_{\kappa}^{*set}$$

2-13

where we recognize that μ_{κ}^{*set} is the set point specific partial Hamiltonian of component κ . In the last term of Equation 2-12, which corresponds to the potential energy of the mass dilation variable, we express the mass dilation variable as $\ln(\eta_{\mu,\kappa})$ instead of $\eta_{\mu,\kappa}$. This results in a Hamiltonian that yields a chemicostat controller of the form

$$\frac{d\zeta_{\mu}}{dt} \propto -m\mu^*(t) + m'\mu^{*set}$$

2-14

We next write the Hamiltonian in the primed frame of reference in terms of the positions and momenta

$$\begin{aligned} H'_{\mu V\mathcal{E}} = & \sum_{\kappa=1}^c \sum_{i=1}^{M_{\kappa}} \sum_{j=1}^{N_{i,\kappa}} \sum_{\alpha=1}^3 \frac{\eta_{\mu,\kappa}}{2} \frac{p'^2_{\alpha,j,i,\kappa}}{m'_{j,i,\kappa}} + \sum_{\kappa=1}^c \sum_{i=1}^{M_{\kappa}} \sum_{j=1}^{N_{i,\kappa}} U_{j,i,\kappa} \\ & + \sum_{\kappa=1}^c \frac{1}{2} \frac{p^2_{\eta,\kappa}}{Q_{\eta,\kappa}} - \sum_{\kappa=1}^c \ln(\eta_{\mu,\kappa}) \mu_{\kappa}^{*set} \sum_{i=1}^{M_{\kappa}} \sum_{j=1}^{N_{i,\kappa}} m'_{j,i,\kappa} \end{aligned}$$

2-15

where $p'_{\alpha,j,i,\kappa}$ is the momentum in the primed frame of reference. This is necessary because it is in these variables that the Hamiltonian and the equations of motion are canonical (or symplectic).

2.2 Derivation of the Equations of Motion

From the Hamiltonian of 2-15, we derive the equations of motion in terms of the laboratory coordinates in the primed frame of reference. Here we rely on the symplectic relationship between the Hamiltonian and the equations of motion:

$$\frac{dr'_{\alpha,j,i,\kappa}}{dt} = \frac{\partial H'_{\mu V\mathcal{E}}}{\partial p'_{\alpha,j,i,\kappa}} = \eta_{\mu,\kappa} \frac{p'_{\alpha,j,i,\kappa}}{m'_{j,i,\kappa}}$$

2-16

$$\frac{dp'_{\alpha,j,i,\kappa}}{dt} = -\frac{\partial H'_{\mu V\mathcal{E}}}{\partial r'_{\alpha,j,i,\kappa}} = -\frac{\partial U_{\alpha,j,i,\kappa}}{\partial r'}$$

2-17

$$\frac{d\eta_{\mu,\kappa}}{dt} = \frac{\partial H'_{\mu V\mathcal{E}}}{\partial p_{\eta,\kappa}} = \frac{p_{\eta,\kappa}}{Q_{\eta,\kappa}}$$

2-18

$$\begin{aligned} \frac{dp_{\eta,\kappa}}{dt} = -\frac{\partial H'_{\mu V \mathcal{E}}}{\partial \eta_{\mu,\kappa}} = & -\sum_{i=1}^{M_\kappa} \sum_{j=1}^{N_{i,\kappa}} \sum_{\alpha=1}^3 \frac{1}{2} \frac{p'^2_{\alpha,j,i,\kappa}}{m'_{j,i,\kappa}} \\ & -\sum_{i=1}^{M_\kappa} \sum_{j=1}^{N_{i,\kappa}} \frac{\partial U_{j,i,\kappa}}{\partial \eta_{\mu,\kappa}} + \frac{\mu_\kappa^{*set}}{\eta_{\mu,\kappa}} \sum_{i=1}^{M_\kappa} \sum_{j=1}^{N_{i,\kappa}} m'_{j,i,\kappa} \end{aligned}$$

2-19

These equations of motion would generate rigorous trajectories themselves, but they are inconvenient since they are in the aphysical (primed) frame of reference. To transform them to the physically meaningful (unprimed) frame of reference, we define a non-canonical transformation.

The first step in performing a non-canonical transformation on the equations of motion is to take the derivative of the transformation equations. The transformation equations are given by 2-20 thru 2-24, and the derivatives of these equations are equations 2-25 thru 2-29:

$$m_{j,i,\kappa} = \eta_{\mu,\kappa} m'_{j,i,\kappa} \tag{2-20}$$

$$p_{\alpha,j,i,\kappa} = \eta_{\mu,\kappa} p'_{\alpha,j,i,\kappa} \tag{2-21}$$

$$r_{\alpha,j,i,\kappa} = r'_{\alpha,j,i,\kappa} \tag{2-22}$$

$$\eta_{\mu,\kappa} = \eta_{\mu,\kappa} \tag{2-23}$$

$$\zeta_{\mu,\kappa} = \frac{p_{\eta,\kappa}}{\eta_{\mu,\kappa} Q_{\eta,\kappa}} \tag{2-24}$$

$$\frac{dm_{j,i,\kappa}}{dt} = m'_{j,i,\kappa} \frac{d\eta_{\mu,\kappa}}{dt} \tag{2-25}$$

$$\frac{dp_{\alpha,j,i,\kappa}}{dt} = \eta_{\mu,\kappa} \frac{dp'_{\alpha,j,i,\kappa}}{dt} + p'_{\alpha,j,i,\kappa} \frac{d\eta_{\mu,\kappa}}{dt}$$

2-26

$$\frac{dr_{\alpha,j,i,\kappa}}{dt} = \frac{dr'_{\alpha,j,i,\kappa}}{dt}$$

2-27

$$\frac{d\eta_{\mu,\kappa}}{dt} = \frac{d\eta_{\mu,\kappa}}{dt}$$

2-28

$$\frac{d\zeta_{\mu,\kappa}}{dt} = \frac{1}{\eta_{\mu,\kappa} Q_{\eta,\kappa}} \frac{dp_{\eta,\kappa}}{dt} - \frac{p_{\eta,\kappa}}{\eta_{\mu,\kappa}^2 Q_{\eta,\kappa}} \frac{d\eta_{\mu,\kappa}}{dt}$$

2-29

The second step of the non-canonical transformation is to substitute the “primed” equations of motion (equations 2-16 to 2-19) into equations 2-25 to 2-29:

$$\frac{dr_{\alpha,j,i,\kappa}}{dt} = \eta_{\mu,\kappa} \frac{p'_{\alpha,j,i,\kappa}}{m'_{j,i,\kappa}}$$

2-30

$$\begin{aligned} \frac{dp_{\alpha,j,i,\kappa}}{dt} &= \eta_{\mu,\kappa} \frac{dp'_{\alpha,j,i,\kappa}}{dt} + p'_{\alpha,j,i,\kappa} \frac{d\eta_{\mu,\kappa}}{dt} \\ &= -\eta_{\mu,\kappa} \frac{\partial U_{\alpha,j,i,\kappa}}{\partial r'} + p'_{\alpha,j,i,\kappa} \left(\frac{p_{\eta,\kappa}}{Q_{\eta,\kappa}} \right) \end{aligned}$$

2-31

$$\frac{d\eta_{\mu,\kappa}}{dt} = \frac{p_{\eta,\kappa}}{Q_{\eta,\kappa}}$$

2-32

$$\begin{aligned}
\frac{d\zeta_{\mu,\kappa}}{dt} &= \frac{1}{\eta_{\mu,\kappa} Q_{\eta,\kappa}} \frac{dp_{\eta,\kappa}}{dt} - \frac{p_{\eta,\kappa}^2}{\eta_{\mu,\kappa}^2 Q_{\eta,\kappa}} \frac{d\eta_{\mu,\kappa}}{dt} \\
&= \frac{1}{\eta_{\mu,\kappa} Q_{\eta,\kappa}} \left(- \sum_{i=1}^{M_\kappa} \sum_{j=1}^{N_{i,\kappa}} \sum_{\alpha=1}^3 \frac{1}{2} \frac{p_{\alpha,j,i,\kappa}'^2}{m_{j,i,\kappa}'} - \sum_{i=1}^{M_\kappa} \sum_{j=1}^{N_{i,\kappa}} \frac{\partial U_{j,i,\kappa}}{\partial \eta_{\mu,\kappa}} \right. \\
&\quad \left. + \frac{\mu_\kappa^{*set}}{\eta_{\mu,\kappa}} \sum_{i=1}^{M_\kappa} \sum_{j=1}^{N_{i,\kappa}} m_{j,i,\kappa}' \right) - \frac{p_{\eta,\kappa}^2}{\eta_{\mu,\kappa}^2 Q_{\eta,\kappa}^2}
\end{aligned}$$

2-33

For the third and final step of the non-canonical transformation, we transform the remaining “primed” variables in equations 2-30 to 2-33 to unprimed physically meaningful variables using the transformation equations 2-20 to 2-24:

$$\frac{dr_{\alpha,j,i,\kappa}}{dt} = \eta_{\mu,\kappa} \frac{p_{\alpha,j,i,\kappa}}{m_{j,i,\kappa}}$$

2-34

$$\frac{dp_{\alpha,j,i,\kappa}}{dt} = -\eta_{\mu,\kappa} \frac{\partial U_{\alpha,j,i,\kappa}}{\partial r} + p_{\alpha,j,i,\kappa} \zeta_{\mu,\kappa}$$

2-35

$$\frac{d\eta_{\mu,\kappa}}{dt} = \zeta_{\mu,\kappa} \eta_{\mu,\kappa}$$

2-36

$$\begin{aligned}
\frac{d\zeta_{\mu,\kappa}}{dt} &= \frac{v_{\mu,\kappa}^2}{\eta_{\mu,\kappa} f k_B T_{set}} \left(- \sum_{i=1}^{M_\kappa} \sum_{j=1}^{N_{i,\kappa}} \sum_{\alpha=1}^3 \frac{1}{2\eta_{\mu,\kappa}} \frac{p_{\alpha,j,i,\kappa}^2}{m_{j,i,\kappa}} - \sum_{i=1}^{M_\kappa} \sum_{j=1}^{N_{i,\kappa}} \frac{\partial U_{j,i,\kappa}}{\partial \eta_{\mu,\kappa}} \right. \\
&\quad \left. + \frac{\mu_\kappa^{*set}}{\eta_{\mu,\kappa}^2} \sum_{i=1}^{M_\kappa} \sum_{j=1}^{N_{i,\kappa}} m_{j,i,\kappa} \right) - \zeta_{\mu,\kappa}^2
\end{aligned}$$

2-37

In the next section, we derive the integration scheme for the equations of motion necessary to perform simulations to test this algorithm.

2.3 Reversible Reference System Propagator Algorithm (rRESPA) Integration Scheme

We will test the μVE EMD algorithm on a simple, monatomic fluid of N particles, using the single time scale reversible reference system propagator algorithm (rRESPA) [13] to integrate numerically the equations of motion. In this section, we show how we derived the rRESPA algorithm for μVE EMD simple fluid simulation.

2.3.1 The Liouville Operator

We begin by simplifying the equations of motion (equations 2-34 to 2-37) and express these for a simple monatomic fluid:

$$\frac{dr_{\alpha,i}}{dt} = \eta_\mu \frac{p_{\alpha,i}}{m_i} \quad 2-38$$

$$\frac{dp_{\alpha,i}}{dt} = -\eta_\mu \frac{\partial U_i}{\partial r_\alpha} + p_{\alpha,i} \zeta_\mu \quad 2-39$$

$$\frac{d\eta_\mu}{dt} = \zeta_\mu \eta_\mu \quad 2-40$$

$$\begin{aligned} \frac{d\zeta_\mu}{dt} = & \frac{v_\mu^2}{\eta_\mu f k_B T_{set}} \left(-\sum_{i=1}^N \sum_{\alpha=1}^3 \frac{1}{2\eta_\mu} \frac{p_{\alpha,i}^2}{m_i} - \sum_{i=1}^N \frac{\partial U_j}{\partial \eta_\mu} \right. \\ & \left. + \frac{1}{\eta_\mu^2} \mu_\kappa^{*set} \sum_{i=1}^N m_i \right) - \zeta_\mu^2 \end{aligned} \quad 2-41$$

Next, we formulate a Liouville operator for the simple monatomic fluid in a μVE system.

The Liouville operator iL for the μVE system is

$$iL = \frac{dr_{\alpha,i}}{dt} \frac{\partial}{\partial r_{\alpha,i}} + \frac{dp_{\alpha,i}}{dt} \frac{\partial}{\partial p_{\alpha,i}} + \frac{d\eta_{\mu,\kappa}}{dt} \frac{\partial}{\partial \eta_{\mu,\kappa}} + \frac{d\zeta_{\mu,\kappa}}{dt} \frac{\partial}{\partial \zeta_{\mu,\kappa}}$$

2-42

This iL operator is split into two parts, iL_1 and iL_2 ,

$$iL = iL_1 + iL_2.$$

2-43

These two parts of the iL operator are arranged as

$$iL = \frac{iL_2}{2} + iL_1 + \frac{iL_2}{2}.$$

2-44

We distribute the terms in equation 2-42 between iL_1 and iL_2 using,

$$iL_1 = \frac{dr_{\alpha,i}}{dt} \frac{\partial}{\partial r_{\alpha,i}}$$

2-45

$$iL_2 = \frac{d\eta_{\mu,\kappa}}{dt} \frac{\partial}{\partial \eta_{\mu,\kappa}} + \frac{dp_{\alpha,i}}{dt} \frac{\partial}{\partial p_{\alpha,i}} + \frac{d\zeta_{\mu,\kappa}}{dt} \frac{\partial}{\partial \zeta_{\mu,\kappa}}$$

2-46

Then we substitute the simplified equations of motion (equations 2-38 to 2-41) into equations 2-45 and 2-46:

$$iL_1 = \frac{dr_{\alpha,i}}{dt} \frac{\partial}{\partial r_{\alpha,i}} = \eta_{\mu} \frac{p_{\alpha,i}}{m_i} \frac{\partial}{\partial r_{\alpha,i}}$$

2-47

$$\begin{aligned} iL_2 &= \frac{d\eta_{\mu}}{dt} \frac{\partial}{\partial \eta_{\mu}} + \frac{dp_{\alpha,i}}{dt} \frac{\partial}{\partial p_{\alpha,i}} + \frac{d\zeta_{\mu}}{dt} \frac{\partial}{\partial \zeta_{\mu}} \\ &= \zeta_{\mu} \eta_{\mu} \frac{\partial}{\partial \eta_{\mu}} + \left(-\frac{\eta_{\mu}}{2} \frac{\partial U_i}{\partial r_{\alpha}} + p_{\alpha,i} \zeta_{\mu} - \frac{\eta_{\mu}}{2} \frac{\partial U_i}{\partial r_{\alpha}} \right) \frac{\partial}{\partial p_{\alpha,i}} \\ &\quad + \left(\frac{v_{\mu}^2}{\eta_{\mu} f k_B T_{set}} \left(-\sum_{i=1}^N \sum_{\alpha=1}^3 \frac{1}{2\eta_{\mu}} \frac{p_{\alpha,i}^2}{m_i} - \sum_{i=1}^N \frac{\partial U_i}{\partial \eta_{\mu}} + \frac{\mu_{\kappa}^{*set}}{\eta_{\mu}^2} \sum_{i=1}^N m_i \right) - \zeta_{\mu}^2 \right) \frac{\partial}{\partial \zeta_{\mu}} \end{aligned}$$

2-48

Finally, we arrive at the final form of our operator:

$$\begin{aligned}
iL = & \frac{1}{2} \left[\left(\frac{\nu_\mu^2}{\eta_\mu f k_B T_{set}} \left(- \sum_{i=1}^N \sum_{\alpha=1}^3 \frac{1}{2\eta_\mu} \frac{p_{\alpha,i}^2}{m_i} - \sum_{i=1}^N \frac{\partial U_i}{\partial \eta_\mu} + \frac{\mu_\kappa^{*set}}{\eta_\mu^2} \sum_{i=1}^N m_i \right) - \zeta_\mu^2 \right) \frac{\partial}{\partial \zeta_\mu} \right. \\
& + \left(- \frac{\eta_\mu}{2} \frac{\partial U_i}{\partial r_\alpha} + p_{\alpha,i} \zeta_\mu - \frac{\eta_\mu}{2} \frac{\partial U_i}{\partial r_\alpha} \right) \frac{\partial}{\partial p_{\alpha,i}} + \zeta_\mu \eta_\mu \frac{\partial}{\partial \eta_\mu} \\
& + \eta_\mu \frac{p_{\alpha,i}}{m_i} \frac{\partial}{\partial r_{\alpha,i}} \\
& \left. + \frac{1}{2} \left[\zeta_\mu \eta_\mu \frac{\partial}{\partial \eta_\mu} + \left(- \frac{\eta_\mu}{2} \frac{\partial U_i}{\partial r_\alpha} + p_{\alpha,i} \zeta_\mu - \frac{\eta_\mu}{2} \frac{\partial U_i}{\partial r_\alpha} \right) \frac{\partial}{\partial p_{\alpha,i}} + \right. \right. \\
& \left. \left(\frac{\nu_\mu^2}{\eta_\mu f k_B T_{set}} \left(- \sum_{i=1}^N \sum_{\alpha=1}^3 \frac{1}{2\eta_\mu} \frac{p_{\alpha,i}^2}{m_i} - \sum_{i=1}^N \frac{\partial U_i}{\partial \eta_\mu} + \frac{\mu_\kappa^{*set}}{\eta_\mu^2} \sum_{i=1}^N m_i \right) - \zeta_\mu^2 \right) \frac{\partial}{\partial \zeta_\mu} \right] \right]
\end{aligned}$$

2-49

We expand equation 2-49, listing the different terms of the operator:

$$\begin{aligned}
iL = & - \frac{1}{2} \zeta_\mu^2 \frac{\partial}{\partial \zeta_\mu} + \frac{1}{2} \frac{\nu_\mu^2}{\eta_\mu f k_B T_{set}} \left(- \sum_{i=1}^N \sum_{\alpha=1}^3 \frac{1}{2\eta_\mu} \frac{p_{\alpha,i}^2}{m_i} - \sum_{i=1}^N \frac{\partial U_i}{\partial \eta_\mu} + \frac{\mu_\kappa^{*set}}{\eta_\mu^2} \sum_{i=1}^N m_i \right) \frac{\partial}{\partial \zeta_\mu} \\
& - \frac{1}{2} \frac{\eta_\mu}{2} \frac{\partial U_i}{\partial r_\alpha} \frac{\partial}{\partial p_{\alpha,i}} + \frac{1}{2} p_{\alpha,i} \zeta_\mu \frac{\partial}{\partial p_{\alpha,i}} - \frac{1}{2} \frac{\eta_\mu}{2} \frac{\partial U_i}{\partial r_\alpha} \frac{\partial}{\partial p_{\alpha,i}} + \frac{1}{2} \zeta_\mu \eta_\mu \frac{\partial}{\partial \eta_\mu} + \eta_\mu \frac{p_{\alpha,i}}{m_i} \frac{\partial}{\partial r_{\alpha,i}} \\
& + \frac{1}{2} \zeta_\mu \eta_\mu \frac{\partial}{\partial \eta_\mu} - \frac{1}{2} \frac{\eta_\mu}{2} \frac{\partial U_i}{\partial r_\alpha} \frac{\partial}{\partial p_{\alpha,i}} + \frac{1}{2} p_{\alpha,i} \zeta_\mu \frac{\partial}{\partial p_{\alpha,i}} - \frac{1}{2} \frac{\eta_\mu}{2} \frac{\partial U_i}{\partial r_\alpha} \frac{\partial}{\partial p_{\alpha,i}} \\
& + \frac{1}{2} \frac{\nu_\mu^2}{\eta_\mu f k_B T_{set}} \left(- \sum_{i=1}^N \sum_{\alpha=1}^3 \frac{1}{2\eta_\mu} \frac{p_{\alpha,i}^2}{m_i} - \sum_{i=1}^N \frac{\partial U_i}{\partial \eta_\mu} + \frac{\mu_\kappa^{*set}}{\eta_\mu^2} \sum_{i=1}^N m_i \right) \frac{\partial}{\partial \zeta_\mu} - \frac{1}{2} \zeta_\mu^2 \frac{\partial}{\partial \zeta_\mu}
\end{aligned}$$

2-50

In the next section we show how this operator is used to obtain the time evolution equations.

2.3.2 The Time Evolution Equations

We use the operator in equation 2-50 on the independent variables p , r , ζ_μ and η_μ to derive the time evolution equations of these quantities. It is important that we apply the terms of the operator in the order shown in equation 2-50 from top to bottom, left to right. In the equations that we derive below, independent variables will have

superscript numbers in parentheses. These numbers represent the computational order at each time step. For example, $\zeta_\mu^{(1)}$ means it is the value of the chemicostat momentum used in the first step of the algorithm, while $\zeta_\mu^{(2)}$ is the value of the chemicostat momentum that will be used in the second step of the algorithm.

We now proceed to derive the rRESPA algorithm. The first and second terms in the operator (2-50) change the chemicostat momentum ζ_μ according to

$$\zeta_\mu^{(2)} = \exp\left(i\left(-\frac{\Delta t}{2}\right)\zeta_\mu^2 \frac{\partial}{\partial \zeta_\mu}\right)\zeta_\mu^{(1)} = \frac{\zeta_\mu^{(1)}}{1 + \frac{\Delta t}{2}\zeta_\mu^{(1)}} \quad \text{2-51}$$

$$\begin{aligned} \zeta_\mu^{(3)} &= \exp\left(i\frac{\Delta t}{2}\frac{\nu_\mu^2}{\eta_\mu f k_B T_{set}}\left(-\sum_{i=1}^N \sum_{\alpha=1}^3 \frac{1}{2\eta_\mu} \frac{p_{\alpha,i}^2}{m_i} - \sum_{i=1}^N \frac{\partial U_i}{\partial \eta_\mu} + \frac{\mu^{*set}}{\eta_\mu^2} \sum_{i=1}^N m_i\right) \frac{\partial}{\partial \zeta_\mu}\right)\zeta_\mu^{(2)} \\ &= \zeta_\mu^{(2)} + \frac{\Delta t}{2}\frac{\nu_\mu^2}{\eta_\mu^{(1)} f k_B T_{set}}\left(-\sum_{i=1}^N \sum_{\alpha=1}^3 \frac{1}{2\eta_\mu^{(1)}} \frac{(p_{\alpha,i}^{(1)})^2}{m_i} - \sum_{i=1}^N \frac{\partial U_i}{\partial \eta_\mu} + \frac{\mu^{*set}}{(\eta_\mu^{(1)})^2} \sum_{i=1}^N m_i\right) \end{aligned} \quad \text{2-52}$$

The third, fourth, and fifth terms of the operator (2-50) change the momentum p according to

$$\begin{aligned} p_{\alpha,i}^{(4)} &= \exp\left(i\frac{\Delta t}{2}\left(-\frac{\eta_\mu}{2}\frac{\partial U_i}{\partial r_\alpha}\right) \frac{\partial}{\partial p_{\alpha,i}}\right)p_{\alpha,i}^{(1)} \\ &= p_{\alpha,i}^{(1)} - \frac{\eta_\mu^{(1)}}{2}\frac{\partial U_i}{\partial r_\alpha} \frac{\Delta t}{2} \end{aligned} \quad \text{2-53}$$

$$\begin{aligned} p_{\alpha,i}^{(5)} &= \exp\left(i\frac{\Delta t}{2}p_{\alpha,i}\zeta_\mu \frac{\partial}{\partial p_{\alpha,i}}\right)p_{\alpha,i}^{(4)} \\ &= p_{\alpha,i}^{(4)} \exp\left(\frac{\Delta t}{2}\zeta_\mu^{(3)}\right) \end{aligned} \quad \text{2-54}$$

$$\begin{aligned}
p_{\alpha,i}^{(6)} &= \exp\left(i\frac{\Delta t}{2}\left(-\frac{\eta_\mu}{2}\frac{\partial U_i}{\partial r_\alpha}\right)\frac{\partial}{\partial p_{\alpha,i}}\right)p_{\alpha,i}^{(5)} \\
&= p_{\alpha,i}^{(5)} - \frac{\eta_\mu^{(1)}}{2}\frac{\partial U_i}{\partial r_\alpha}\frac{\Delta t}{2}
\end{aligned}$$

2-55

The sixth term of the operator (2-50) changes the mass dilation variable η_μ using

$$\begin{aligned}
\eta_\mu^{(7)} &= \exp\left(i\frac{\Delta t}{2}\zeta_\mu\eta_\mu\frac{\partial}{\partial \eta_\mu}\right)\eta_\mu^{(1)} \\
&= \eta_\mu^{(1)}\exp\left(\frac{\Delta t}{2}\zeta_\mu^{(3)}\right)
\end{aligned}$$

2-56

The seventh term of the operator (2-50) changes the position \mathbf{r} :

$$\begin{aligned}
r_{\alpha,i}^{(8)} &= \exp\left(i\Delta t\eta_\mu\frac{p_{\alpha,i}}{m_i}\frac{\partial}{\partial r_{\alpha,i}}\right)r_{\alpha,i}^{(1)} \\
&= r_i^{(1)} + \Delta t\eta_\mu^{(7)}\frac{p_{\alpha,i}^{(6)}}{m_i}
\end{aligned}$$

2-57

The eighth term of the operator (2-50) changes the mass dilation variable η_μ :

$$\begin{aligned}
\eta_\mu^{(9)} &= \exp\left(i\frac{\Delta t}{2}\zeta_\mu\eta_\mu\frac{\partial}{\partial \eta_{\mu,\kappa}}\right)\eta_\mu^{(7)} \\
&= \eta_\mu^{(7)}\exp\left(\frac{\Delta t}{2}\zeta_\mu^{(3)}\right)
\end{aligned}$$

2-58

The ninth, tenth, and eleventh terms of the operator (2-50) will change the momentum, \mathbf{p} :

$$\begin{aligned}
p_{\alpha,i}^{(10)} &= \exp\left(i\frac{\Delta t}{2}\left(-\frac{\eta_\mu}{2}\frac{\partial U_i}{\partial r_\alpha}\right)\frac{\partial}{\partial p_{\alpha,i}}\right)p_{\alpha,i}^{(6)} \\
&= p_{\alpha,i}^{(6)} - \frac{\eta_\mu^{(9)}}{2}\frac{\partial U_i}{\partial r_\alpha}\frac{\Delta t}{2}
\end{aligned}$$

2-59

$$\begin{aligned}
p_{\alpha,i}^{(11)} &= \exp\left(i \frac{\Delta t}{2} p_{\alpha,i} \zeta_\mu \frac{\partial}{\partial p_{\alpha,i}}\right) p_{\alpha,i}^{(10)} \\
&= p_{\alpha,i}^{(10)} \exp\left(\frac{\Delta t}{2} \zeta_\mu^{(3)}\right)
\end{aligned}$$

2-60

$$\begin{aligned}
p_{\alpha,i}^{(12)} &= \exp\left(i \frac{\Delta t}{2} \left(-\frac{\eta_\mu}{2} \frac{\partial U_i}{\partial r_\alpha}\right) \frac{\partial}{\partial p_{\alpha,i}}\right) p_{\alpha,i}^{(11)} \\
&= p_{\alpha,i}^{(11)} - \frac{\eta_\mu^{(9)}}{2} \frac{\partial U_i}{\partial r_\alpha} \frac{\Delta t}{2}
\end{aligned}$$

2-61

The twelfth and thirteenth terms of the operator (2-50) will change the chemicostat momentum ζ_μ according to

$$\begin{aligned}
\zeta_\mu^{(13)} &= \exp\left(i \frac{\Delta t}{2} \frac{v_\mu^2}{\eta_\mu f k_B T_{set}} \left(-\sum_{i=1}^N \sum_{\alpha=1}^3 \frac{1}{2\eta_\mu} \frac{p_{\alpha,i}^2}{m_i} - \sum_{i=1}^N \frac{\partial U_i}{\partial \eta_\mu} + \frac{\mu^{*set}}{\eta_\mu^2} \sum_{i=1}^N m_i\right) \frac{\partial}{\partial \zeta_\mu}\right) \zeta_\mu^{(3)} \\
&= \zeta_\mu^{(3)} + \frac{\Delta t}{2} \frac{v_\mu^2}{\eta_\mu^{(9)} f k_B T_{set}} \left(-\sum_{i=1}^N \sum_{\alpha=1}^3 \frac{1}{2\eta_\mu^{(9)}} \frac{(p_{\alpha,i}^{(12)})^2}{m_i} - \sum_{i=1}^N \frac{\partial U_i}{\partial \eta_\mu} + \frac{\mu^{*set}}{(\eta_\mu^{(9)})^2} \sum_{i=1}^N m_i\right)
\end{aligned}$$

2-62

$$\zeta_\mu^{(14)} = \exp\left(i \left(-\frac{\Delta t}{2}\right) \zeta_\mu^2 \frac{\partial}{\partial \zeta_\mu}\right) \zeta_\mu^{(13)} = \frac{\zeta_\mu^{(13)}}{1 + \frac{\Delta t}{2} \zeta_\mu^{(13)}}$$

2-63

We give a summary of the rRESPA algorithm below. This algorithm was used in simulations presented in the next chapter.

2.3.3 rRESPA Algorithm

Before we begin the integration scheme, we compute the forces between particles based on the current positions of the particles. Following the computation of forces, the integration scheme begins with the chemicostat momentum:

$$\zeta_{\mu}^{(2)} = \frac{\zeta_{\mu}^{(1)}}{1 + \frac{\Delta t}{2} \zeta_{\mu}^{(1)}}$$

2-64

$$\mu^*(t) = \frac{1}{N} \left(\frac{1}{2} \sum_{\alpha=1}^3 \sum_{i=1}^N v_{i,\alpha}^2 + \sum_{i=1}^N \frac{\partial U_i}{\partial m_i} \right)$$

2-65

$$\begin{aligned} \zeta_{\mu}^{(3)} = \zeta_{\mu}^{(2)} + \frac{\Delta t}{2} \frac{v_{\mu}^2}{\eta_{\mu}^{(1)} f k_B T_{set}} & \left(- \sum_{i=1}^N \sum_{\alpha=1}^3 \frac{1}{2 \eta_{\mu}^{(1)}} \frac{(p_{\alpha,i}^{(1)})^2}{m_i} - \sum_{i=1}^N \frac{\partial U_i}{\partial \eta_{\mu}} \right. \\ & \left. + \frac{\mu_{\kappa}^{*set}}{(\eta_{\mu}^{(1)})^2} \sum_{i=1}^N m_i \right) \end{aligned}$$

2-66

We substitute some terms in equation 2-66 with the instantaneous partial specific Hamiltonian of 2-65. For a monatomic simple fluid, m_i is constant and can be factored out and 2-66 then simplifies to 2-67

$$\zeta_{\mu}^{(3)} = \zeta_{\mu}^{(2)} + \frac{\Delta t}{2} \frac{v_{\mu}^2}{f k_B T_{set}} \frac{1}{(\eta_{\mu}^{(1)})^2} M \left(-\mu^*(t) m_i + \mu^{*set} m_i' \right)$$

2-67

Next, we solve for the momenta, p_i :

$$p_{\alpha,i}^{(4)} = p_{\alpha,i}^{(1)} - \frac{\eta_{\mu}^{(1)}}{2} \frac{\partial U_i}{\partial r_{\alpha}} \frac{\Delta t}{2}$$

2-68

$$p_{\alpha,i}^{(5)} = p_{\alpha,i}^{(4)} \exp \left(\frac{\Delta t}{2} \zeta_{\mu}^{(3)} \right)$$

2-69

$$p_{\alpha,i}^{(6)} = p_{\alpha,i}^{(5)} - \frac{\eta_{\mu}^{(1)}}{2} \frac{\partial U_i}{\partial r_{\alpha}} \frac{\Delta t}{2}$$

2-70

When equations 2-68 through 2-70 are combined, we get the equation

$$p_{\alpha,i}^{(6)} = \left(p_{\alpha,i}^{(3)} - \frac{\eta_{\mu}^{(1)}}{2} \frac{\partial U_i}{\partial r_{\alpha}} \frac{\Delta t}{2} \right) \exp\left(\frac{\Delta t}{2} \zeta_{\mu}^{(3)}\right) - \frac{\eta_{\mu}^{(1)}}{2} \frac{\partial U_i}{\partial r_{\alpha}} \frac{\Delta t}{2}$$

2-71

The momentum equation can also be expressed in terms of the force, F_i , as

$$F_{i,\alpha} = -\frac{\partial U_i}{\partial r_{\alpha}}$$

2-72

Substituting 2-72 into 2-71, we arrive at the following expression for momenta p_i :

$$p_{\alpha,i}^{(6)} = \left(p_{\alpha,i}^{(3)} + F_{i,\alpha} \frac{\eta_{\mu}^{(1)}}{2} \frac{\Delta t}{2} \right) \exp\left(\frac{\Delta t}{2} \zeta_{\mu}^{(3)}\right) + F_{i,\alpha} \frac{\eta_{\mu}^{(1)}}{2} \frac{\Delta t}{2}$$

2-73

Next, we calculate the new value of the mass dilation variable η_{μ} according to

$$\eta_{\mu}^{(7)} = \eta_{\mu}^{(1)} \exp\left(\frac{\Delta t}{2} \zeta_{\mu}^{(3)}\right)$$

2-74

Then we calculate the new positions of the particles as

$$r_{\alpha,i}^{(8)} = r_i^{(1)} + \Delta t \eta_{\mu}^{(7)} \frac{p_{\alpha,i}^{(6)}}{m_i}$$

2-75

Since we have new positions for the particles, we calculate the new forces between the particles. We proceed to calculating the new mass dilation variable η_{μ} as

$$\eta_{\mu}^{(9)} = \eta_{\mu}^{(7)} \exp\left(\frac{\Delta t}{2} \zeta_{\mu}^{(3)}\right)$$

2-76

Then we compute for the new momenta of the particles

$$p_{\alpha,i}^{(12)} = \left(p_{\alpha,i}^{(10)} + F_{i,\alpha} \frac{\eta_{\mu}^{(9)}}{2} \frac{\Delta t}{2} \right) \exp\left(\frac{\Delta t}{2} \zeta_{\mu}^{(3)}\right) + F_{i,\alpha} \frac{\eta_{\mu}^{(9)}}{2} \frac{\Delta t}{2}$$

2-77

Finally, we calculate the chemicostat momentum ζ_μ according to

$$\zeta_\mu^{(13)} = \zeta_\mu^{(3)} + \frac{\Delta t}{2} \frac{v_\mu^2}{f k_B T_{set}} \frac{1}{(\eta_\mu^{(9)})^2} M m_i (-\mu^*(t) m_i + \mu^{*set} m'_i)$$

2-78

$$\zeta_\mu^{(14)} = \frac{\zeta_\mu^{(13)}}{1 + \frac{\Delta t}{2} \zeta_\mu^{(13)}}$$

2-79

We use the integration algorithm summarized above in our $\mu\text{V}\mathcal{E}$ simulations.

3 $\mu V\mathcal{E}$ Ensemble Simulations

We ran simulations using the algorithm derived in Chapter 2 for a monatomic simple fluid. First, we tested whether the chemicostat functioned properly, *i.e.*, it should drive the system towards the set point product of the partial specific Hamiltonian and mass. We then evaluated the simulation results to determine whether the simulation was truly in the $\mu V\mathcal{E}$ ensemble.

The algorithm was first tested for the simplest system – an ideal gas, where potential energy is negligible. Then the algorithm was tested on a dilute gas, a system that has potential energy. Two types of simulation were run with the dilute gas system. In the first type of simulation, the potential energy was expressed as a product of the mass and the specific potential energy, $m\hat{U}$. In the second type of simulation, the potential energy was expressed as a function of both the distance between particles and the number density, $U(\mathbf{r}, \rho)$.

3.1 $\mu V\mathcal{E}$ Ideal Gas

For an ideal gas, the Hamiltonian in equation 2-15 reduces to equation 3-1:

$$H'_{\mu V\mathcal{E}} = \sum_{i=1}^N \sum_{\alpha=1}^3 \frac{\eta_{\mu,\kappa}}{2} \frac{p'^2_{\alpha,i}}{m'_i} + \frac{1}{2} \frac{p^2_{\eta}}{Q_{\eta}} - \ln(\eta_{\mu}) \mu^{set} \sum_{i=1}^N m'_i$$

3-1

The equations of motion are derived canonically from the Hamiltonian in the primed frame of reference. This is followed by a noncanonical transformation of the equations of motion from the primed frame of reference to the physical or unprimed frame of reference. The derivation is similar to the procedure illustrated in Chapter 2. Below are the equations of motion derived from the Hamiltonian 3-1:

$$\frac{dr_{\alpha,i}}{dt} = \eta_{\mu} \frac{p_{\alpha,i}}{m_i} \quad 3-2$$

$$\frac{dp_{\alpha,i}}{dt} = p_{\alpha,i} \zeta_{\mu} \quad 3-3$$

$$\frac{d\eta_{\mu}}{dt} = \zeta_{\mu} \eta_{\mu} \quad 3-4$$

$$\frac{d\zeta_{\mu}}{dt} = \frac{N}{\eta_{\mu}^2 Q_{\eta}} \left(-\mu(t)m_i + \mu^{set} m_i' \right) - \zeta_{\mu}^2 \quad 3-5$$

The partial specific Hamiltonian for this ideal gas system only has the kinetic energy term, since potential energy is negligible. It is a function of the particle velocities.

$$\mu^*(t) = \sum_{i=1}^N \sum_{\alpha=1}^3 \frac{1}{2N} \frac{p_{\alpha,i}^2}{m_i^2} \quad \text{or} \quad \mu^*(t) = \sum_{i=1}^N \sum_{\alpha=1}^3 \frac{1}{2N} v_{\alpha,i}^2 \quad 3-6$$

If we derive the evolution equation for the velocity, we see that the velocity does not change in time, as shown in the derivation

$$\begin{aligned} p &= mv \\ \frac{dp}{dt} &= v \frac{dm}{dt} + m \frac{dv}{dt} \\ \frac{dv}{dt} &= \frac{1}{m} \frac{dp}{dt} - \frac{v}{m} \frac{dm}{dt} \\ \frac{dv}{dt} &= \frac{1}{m} p \zeta_{\mu} - \frac{v}{m} m' \eta_{\mu} \zeta_{\mu} \\ \frac{dv}{dt} &= 0 \end{aligned} \quad 3-7$$

Since the velocity will never change $\mu^*(t)$ will not change. Using the equations of motion (3-2 to 3-5), we simulate a monatomic simple fluid. The simulation system properties are summarized in Table 3.1–1.

Table 3.1-1 Simulation Input Parameters for Methane

	Value	Reduced Value
Mass	2.6568 grams/molecule	1.0
Sigma	3.780 Angstroms	1.0
Epsilon	2.1262 Joules	1.0
Temperature	335 Kelvin	2.1752
Density	2.6772E-5 particles/Angstrom ³	1.446E-3
Δt	2 femtoseconds	1.372E-3
Length of simulation	2 to 3 million steps or 4 to 6 nanoseconds	
Number of particles	4000	

3.1.1 Simulation where μ^{*set} is Equal to $\mu^*(t_o)$

We first run a simulation where the set point partial specific Hamiltonian is equal to the initial value of the partial specific Hamiltonian ($\mu^{*set} = \mu^*(t_o)$). In this case, since we are simulating an ideal gas, the partial specific Hamiltonian will remain at a constant value through out the simulation. The partial specific Hamiltonian will be equal to the set point throughout the simulation and the chemicostat controller is not expected to react.

The initial value for the partial specific Hamiltonian $\mu^*(t_o)$ is 3.2628, which is also our set point partial specific Hamiltonian, μ^{*set} . To obtain the partial specific Hamiltonian we run the simulation until the system reaches equilibrium and we read off the value for the partial specific Hamiltonian.

As predicted, the chemicostat controller did not react since there was never a time when $\mu^{*set} \neq \mu^*(t_o)$. In Figure 3.1-1, we show that the mass remained constant and in Figure 3.1-2, that the product $\mu^*(t)m$ did not change; it remained at the set point $\mu^{*set} m'$ value of 3.2628. This base case thus produced reasonable results as predicted.

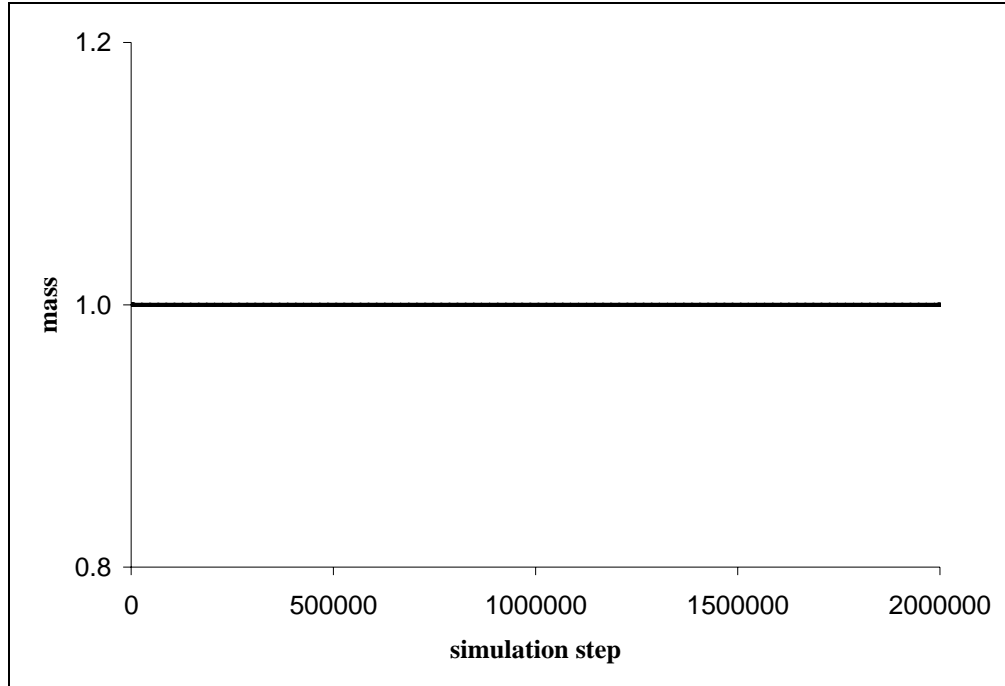


Figure 3.1-1 Mass vs. simulation steps for an ideal gas system, with $\mu^{*set} = \mu^*(t_o)$.

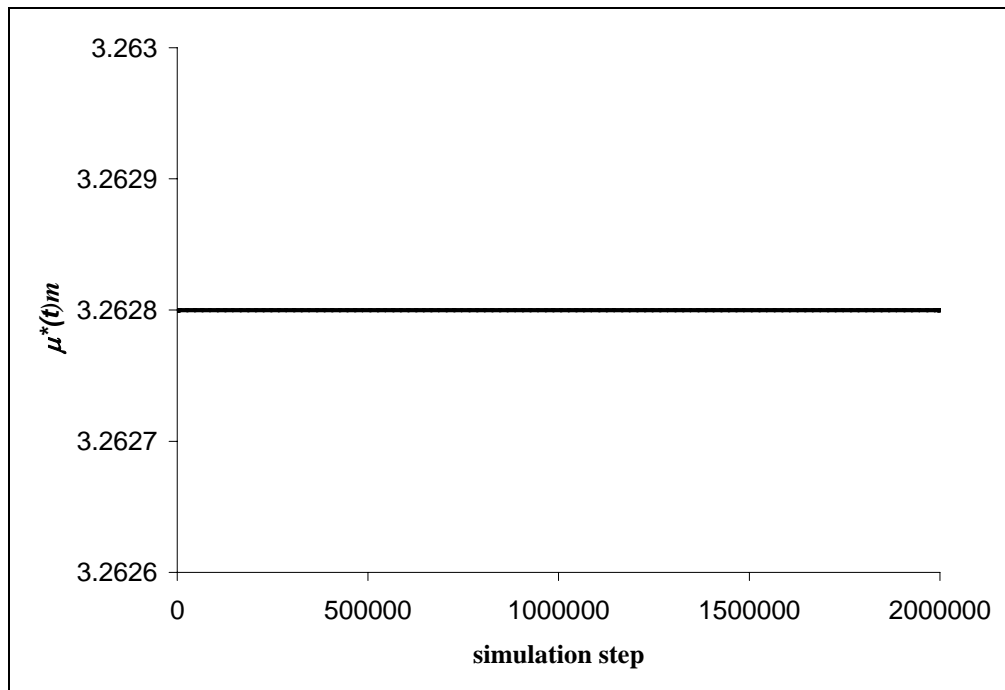


Figure 3.1-2 $\mu^*(t)m$ vs. simulation steps for an ideal gas system, with $\mu^{*set} = \mu^*(t_o)$.

3.1.2 Simulation where $\mu^{*set} < \mu^*(t_0)$

In the case where μ^{*set} is less than $\mu^*(t_0)$, $\mu^*(t)$ will still remain constant since this is still an ideal gas simulation but the chemicostat controller is expected to react and drive $\mu^*(t)m$ towards $\mu^{*set} m'$. The product $\mu^{*set} m'$ was set equal to 3.262 (slightly less than 3.2628). Figure 3.1-3 shows that $\mu^*(t)$ is constant at 3.2628 throughout the simulation. We can see that the controller drives $\mu^*(t)m$ toward the set point in Figure 3.1-4. The product $\mu^*(t)m$ fluctuates about the set point; it has an average and standard deviation value of 3.262000 ± 0.000016 . The mass adjusted its value (Figure 3.1-5), from 1.0 to the simulation average mass of 0.999755 ± 0.000005 .

Thus the chemicostat controller is functioning properly for the ideal gas system based on the initial tests of the $\mu V\mathcal{E}$ algorithm. The following sections describe dilute gas simulations.

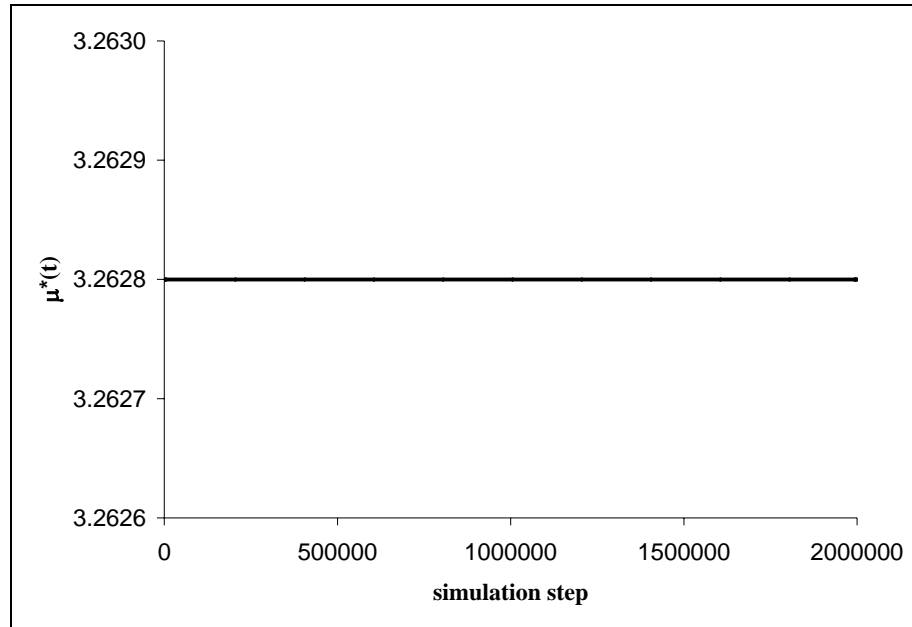


Figure 3.1-3 $\mu^*(t)$ vs. simulation step for an ideal gas system, with $\mu^{*set}=3.262$.

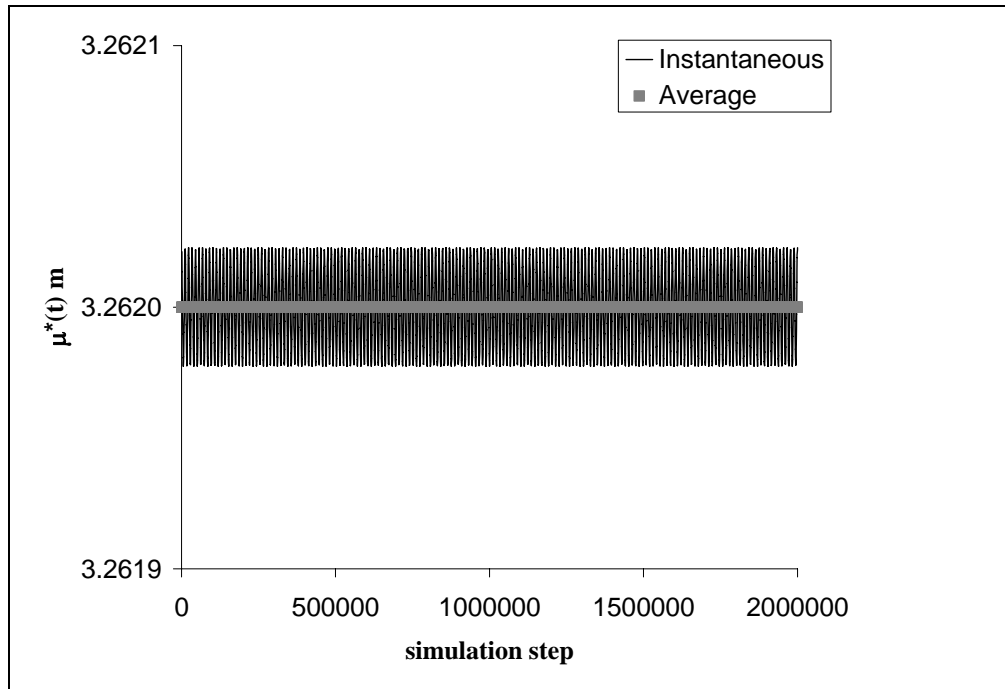


Figure 3.1-4 $\mu^*(t)m$ vs. simulation step for an ideal gas system, with $\mu^{*set}=3.262$.

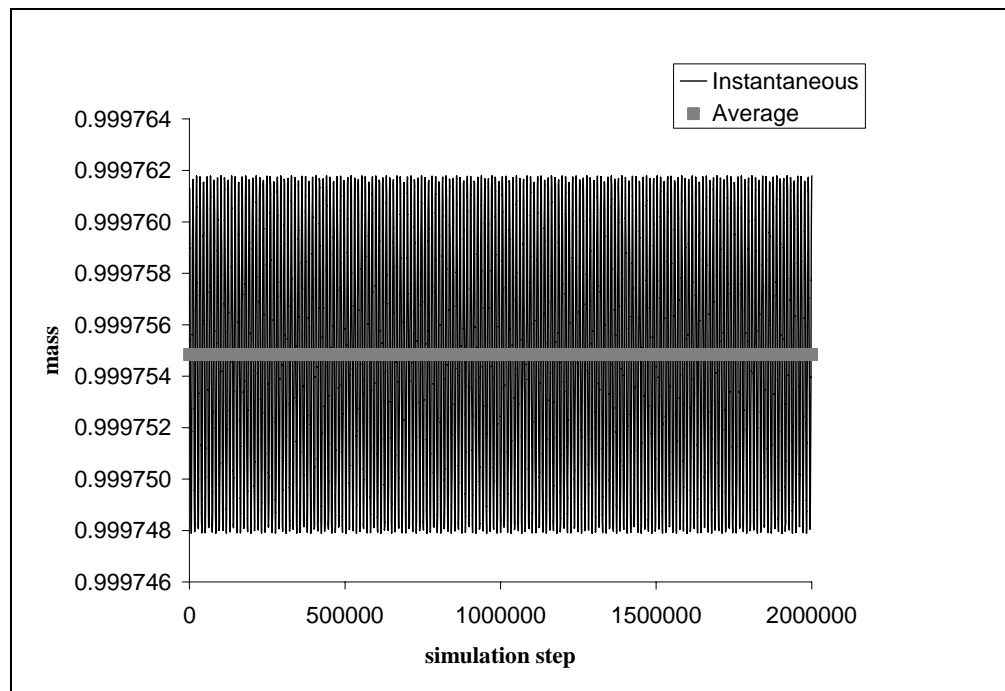


Figure 3.1-5 Mass vs. simulation step for an ideal gas system, with $\mu^{*set}=3.262$.

3.2 Dilute Gas Simulations, Forms of the Potential Energy

In the simulation of simple fluids, the potential energy is normally expressed as a function of the distances between particles, such as the pairwise interaction potential known as the Lennard-Jones potential energy. In a system where the chemical potential, or in our case, the partial specific Hamiltonian, is held constant, the potential energy of the system should change as the number of particles within the system changes. For our simulation, where mass is dilated instead of changing the number of particles in the system, the potential energy has to adjust accordingly. Thus, an expression for the potential energy as a function of mass is needed.

We clarify some terms before we proceed to discuss the two forms for the potential energy used in our dilute gas simulations. In a one component system, the total mass M is equal to Nm , where N is the total number of particles in the system. We divide the total mass with the undilated mass, m' , to get the relationship between the number of particles in the physical frame of reference and the primed frame of reference,

$$N' = \frac{M}{m'} = \frac{Nm}{m'} = N\eta_\mu \quad 3-8$$

where N is the constant number of particles in the unprimed frame of reference and N' is the effective number of particles. The effective number density is

$$\rho' = \frac{N\eta_\mu}{V} \quad 3-9$$

3.2.1 The Specific Potential Energy

The potential energy can be expressed in terms of the mass of a particle multiplied by the specific potential energy,

$$U_i = m\hat{U}_i \quad 3-10$$

where \hat{U}_i is the potential energy for particle i on a specific (per unit mass) basis. We define the instantaneous specific potential energy as,

$$\hat{U}(r_{ij}) = 4 \frac{\varepsilon}{m'} \left[\left(\frac{\sigma}{r_{ij}} \right)^{12} - \left(\frac{\sigma}{r_{ij}} \right)^6 \right]$$

3-11

There is an additional $1/m'$ term in equation 3-11 to remove any mass dependence. Since \hat{U} is independent of mass, it should not be affected by changes in the mass dilation variable.

In our derivations in Chapter 2, we used a general expression for the potential energy U . We present below the equations that have the potential energy term U expressed as the product of the mass and the specific potential energy $m\hat{U}_i$.

First, we have the equation for the NVE Hamiltonian (from equation 2-10) and the partial specific Hamiltonian (from equation 2-11):

$$H_{NVE} = \sum_{i=1}^N m \left[\frac{1}{2} \sum_{\alpha=1}^3 v_{i,\alpha}^2 + \hat{U}_i(\mathbf{r}) \right]$$

3-12

$$\mu_{\kappa}^*(t) = \sum_{i=1}^N \left[\frac{1}{2} \sum_{\alpha=1}^3 v_{i,\alpha}^2 + \hat{U}_i(\mathbf{r}) \right] = \frac{H_{NVE}}{Nm}$$

3-13

Next is the $\mu V \mathcal{E}$ Hamiltonian (from equation 2-15) expressed in the primed frame of reference,

$$\begin{aligned} H'_{\mu V \mathcal{E}} = & \sum_{\kappa=1}^c \sum_{i=1}^{M_{\kappa}} \sum_{j=1}^{N_{i,\kappa}} \sum_{\alpha=1}^3 \frac{\eta_{\mu,\kappa}}{2} \frac{p'^2_{\alpha,j,i,\kappa}}{m'_{j,i,\kappa}} + \sum_{\kappa=1}^c \sum_{i=1}^{M_{\kappa}} \sum_{j=1}^{N_{i,\kappa}} \eta_{\mu,\kappa} m'_{j,i,\kappa} \hat{U}_{j,i,\kappa}(r') \\ & + \sum_{\kappa=1}^c \frac{1}{2} \frac{p^2_{\eta,\kappa}}{Q_{\eta,\kappa}} - \sum_{\kappa=1}^c \ln(\eta_{\mu,\kappa}) \mu_{\kappa}^{set} \sum_{i=1}^{M_{\kappa}} \sum_{j=1}^{N_{i,\kappa}} m'_{j,i,\kappa} \end{aligned}$$

3-14

Last, we have the equations of motion for the momentum (equations 2-17 and 2-35 are transformed to equations 3-15 and 3-16, respectively) and the chemicostat momentum (equations 2-19 and 2-37 are transformed to equations 3-17 and 3-18, respectively). We now present the equations of motion in the primed frame of reference in simplified form for a monatomic simple fluid in the unprimed frame of reference:

$$\frac{dp'_{\alpha,j,i,\kappa}}{dt} = -\frac{\partial H'_{\mu V\mathcal{E}}}{\partial r'_{\alpha,j,i,\kappa}} = -\eta_{\mu,\kappa} m'_{j,i,\kappa} \frac{\partial \hat{U}_{\alpha,j,i,\kappa}(\mathbf{r}')}{\partial \mathbf{r}'} \quad 3-15$$

$$\frac{dp_{\alpha,i}}{dt} = -\eta_{\mu} m'_i \frac{\partial \hat{U}_{\alpha,i}(\mathbf{r})}{\partial \mathbf{r}} + p_{\alpha,i} \zeta_{\mu} \quad 3-16$$

$$\begin{aligned} \frac{dp_{\eta,\kappa}}{dt'} = -\frac{\partial H'_{\mu V\mathcal{E}}}{\partial \eta_{\eta,\kappa}} = & -\sum_{i=1}^{M_{\kappa}} \sum_{j=1}^{N_{i,\kappa}} \sum_{\alpha=1}^3 \frac{1}{2} \frac{p'^2_{\alpha,j,i,\kappa}}{m'_{j,i,\kappa}} \\ & - \sum_{i=1}^{M_{\kappa}} \sum_{j=1}^{N_{i,\kappa}} m'_{j,i,\kappa} \hat{U}_{j,i,\kappa}(\mathbf{r}') + \mu_{\kappa}^{*set} \sum_{i=1}^{M_{\kappa}} \sum_{j=1}^{N_{i,\kappa}} m'_{j,i,\kappa} \end{aligned} \quad 3-17$$

$$\frac{d\zeta_{\mu}}{dt} = \frac{v_{\mu}^2}{\eta_{\mu} f k_B T_{set}} \left(-\sum_{i=1}^N \sum_{\alpha=1}^3 \frac{1}{2\eta_{\mu}} \frac{p^2_{\alpha,i}}{m_i} - \sum_{i=1}^N \frac{m_i}{\eta_{\mu}} \hat{U}_i(\mathbf{r}) + \frac{1}{\eta_{\mu}} \mu^{*set} \sum_{i=1}^N m_i \right) - \zeta_{\mu}^2 \quad 3-18$$

3.2.2 Potential Energy as a Function of \mathbf{r} and ρ

The potential energy can also be expressed as a function of the distance between particles and the number density of the system. As mentioned previously, the potential energy can be given in terms of a pair-wise interaction potential in a simple system, such as the Lennard-Jones potential energy.

$$U = \frac{1}{2} \sum_{i=1}^N \sum_{\substack{j=1 \\ j \neq i}}^N u(r_{ij}) \quad 3-19$$

We also know that the energy of the system can be expressed through the pair correlation function, $g(r)$, as

$$\bar{U} = \sum_{i=1}^N \frac{1}{2} \frac{N}{V} \int_0^{\infty} u(r) g(r) 4\pi r^2 dr \quad 3-20$$

where \bar{U} is the statistical mechanical mean potential energy. Since all N particles are identical, this can also be written as

$$\bar{U} = \frac{1}{2} \frac{N^2}{V} \int_0^\infty u(r) g(r) 4\pi r^2 dr$$

3-21

To arrive at an expression for the instantaneous potential energy, we begin with defining an instantaneous pair correlation function. At any instant in time, we can define an instantaneous pair correlation function about particle i , given by

$$g(r_{ij}, t) = \sum_{\substack{j=1 \\ j \neq i}}^N \frac{1}{\rho 4\pi r_{ij}^2} \delta(r_{ij}(t))$$

3-22

where we are now explicitly indicating the time dependence of the instantaneous pair correlation function, $g(r, t)$. We can see that this expression for $g(r, t)$ is valid because it satisfies the definition of the pair correlation function,

$$\rho \int_0^\infty g(r) 4\pi r^2 dr \equiv N - 1$$

3-23

This pair correlation function is also written as a function of the number density. To introduce a density dependence into the pair correlation function, we write it as

$$g(r, \rho) = g(r, \rho) \frac{g(r, \rho(t)_{\text{effective}})}{g(r, \rho)}$$

3-24

The first term on the RHS of equation 3-24 is the pair correlation function at the particle density of the system; this density is constant. The term $\rho(t)_{\text{effective}}$ is the effective particle density, ρ' . The second term is the ratio of heights in the pair correlation function at different densities. Effectively, it weights the interaction according to a different density. We then replace only the first pair correlation function with the instantaneous pair correlation function,

$$g(r, \rho) = \sum_{\substack{j=1 \\ j \neq i}}^N \frac{1}{\rho 4\pi r_{ij}^2} \delta(r_{ij}(t)) \frac{g(r, \rho(t)_{\text{effective}})}{g(r, \rho)}$$

3-25

Thus the instantaneous potential energy as a function of the distance between particles and the number density is

$$U(r, \rho) = \frac{1}{2} \sum_{i=1}^N \sum_{\substack{j=1 \\ j \neq i}}^N u(r_{ij}(t)) \frac{g(r_{ij}(t), \rho(t)_{effective})}{g(r_{ij}(t), \rho)}$$

3-26

The effective average potential energy at the average effective system density is given by:

$$\bar{U}(r, \rho) = \frac{|\rho_{effective}|}{\rho} \left| \frac{1}{2} \sum_{i=1}^N \sum_{\substack{j=1 \\ j \neq i}}^N u(r_{ij}(t)) \frac{g(r_{ij}(t), \rho(t)_{effective})}{g(r_{ij}(t), \rho)} \right|$$

3-27

In our derivations in Chapter 2, we used a general expression for the potential energy U . We show below the equations that have the potential energy term U expressed as $U(\mathbf{r}, \rho)$. First, we have the equation for the NVE Hamiltonian (from equation 2-10) and the partial specific Hamiltonian (from equation 2-11):

$$H_{NVE} = \frac{1}{2} \sum_{\alpha=1}^3 \sum_{i=1}^N m v_{i,\alpha}^2 + \sum_{i=1}^N U_i(\mathbf{r}, \rho)$$

3-28

$$\begin{aligned} \mu^*(t) &= \frac{1}{N} \left(\frac{1}{2} \sum_{\alpha=1}^3 \sum_{i=1}^N v_{i,\alpha}^2 + \sum_{i=1}^N \frac{\partial U_i(\mathbf{r}, \rho)}{\partial m} \right) \\ &= \frac{1}{N} \left(\frac{1}{2} \sum_{\alpha=1}^3 \sum_{i=1}^N v_{i,\alpha}^2 + \sum_{i=1}^N \frac{\partial U_i(\mathbf{r}, \rho)}{m' \partial \eta_\mu} \right) \end{aligned}$$

3-29

Next is the $\mu V\mathcal{E}$ Hamiltonian (from equation 2-15) expressed in the primed frame of reference,

$$\begin{aligned} H'_{\mu V\mathcal{E}} &= \sum_{\kappa=1}^c \sum_{i=1}^{M_\kappa} \sum_{j=1}^{N_{i,\kappa}} \sum_{\alpha=1}^3 \frac{\eta_{\mu,\kappa}}{2} \frac{p'^2_{\alpha,j,i,\kappa}}{m'_{j,i,\kappa}} + \sum_{\kappa=1}^c \sum_{i=1}^{M_\kappa} \sum_{j=1}^{N_{i,\kappa}} U_{j,i,\kappa}(\mathbf{r}', \rho') \\ &+ \sum_{\kappa=1}^c \frac{1}{2} \frac{p_{\eta,\kappa}^2}{Q_{\eta,\kappa}} - \sum_{\kappa=1}^c \ln(\eta_{\mu,\kappa}) \mu_\kappa^{*set} \sum_{i=1}^{M_\kappa} \sum_{j=1}^{N_{i,\kappa}} m'_{j,i,\kappa} \end{aligned}$$

3-30

Last, we have the equations of motion for the momentum (equations 2-17 and 2-35 are transformed to equations 3-31 and 3-32, respectively) and the chemicostat momentum (equations 2-19 and 2-37 are transformed to equations 3-33 and 3-34). We present the

equations of motion in the primed frame of reference and its simplified form for a monatomic simple fluid in the unprimed frame of reference:

$$\frac{dp'_{\alpha,j,i,\kappa}}{dt} = -\frac{\partial H'_{\mu V\mathcal{E}}}{\partial r'_{\alpha,j,i,\kappa}} = -\frac{\partial U_{\alpha,j,i,\kappa}(\mathbf{r}', \rho')}{\partial r'} \quad 3-31$$

$$\frac{dp_{\alpha,i}}{dt} = -\eta_{\mu} \frac{\partial U_{\alpha,i}(\mathbf{r}, \rho)}{\partial r} + p_{\alpha,i} \zeta_{\mu} \quad 3-32$$

$$\begin{aligned} \frac{dp_{\eta,\kappa}}{dt} = -\frac{\partial H'_{\mu V\mathcal{E}}}{\partial \eta_{\mu,\kappa}} = & -\sum_{i=1}^{M_{\kappa}} \sum_{j=1}^{N_{i,\kappa}} \sum_{\alpha=1}^3 \frac{1}{2} \frac{p'^2_{\alpha,j,i,\kappa}}{m'_{j,i,\kappa}} \\ & - \sum_{i=1}^{M_{\kappa}} \sum_{j=1}^{N_{i,\kappa}} \frac{\partial U_{j,i,\kappa}(\mathbf{r}', \rho')}{\partial \eta_{\mu,\kappa}} + \mu_{\kappa}^{*set} \sum_{i=1}^{M_{\kappa}} \sum_{j=1}^{N_{i,\kappa}} m'_{j,i,\kappa} \end{aligned} \quad 3-33$$

$$\begin{aligned} \frac{d\zeta_{\mu}}{dt} = & \frac{v_{\mu}^2}{\eta_{\mu} f k_B T_{set}} \left(-\sum_{i=1}^N \sum_{\alpha=1}^3 \frac{1}{2\eta_{\mu}} \frac{p^2_{\alpha,i}}{m_i} - \sum_{i=1}^N \frac{\partial U_i(\mathbf{r}, \rho)}{\partial \eta_{\mu}} \right. \\ & \left. + \frac{\mu^{*set}}{\eta_{\mu}} \sum_{i=1}^N m_i \right) - \zeta_{\mu}^2 \end{aligned} \quad 3-34$$

3.3 $\mu V\mathcal{E}$ Dilute Gas Simulations Using the Specific Potential Energy

Using the same system in Table 3.1–1, we first ran simulations where we specified μ^{*set} to be equal $\mu^{*}(t_o)$. The simulation resulted in a rapidly increasing value of $\mu^{*}(t)$, as shown in Figure 3.3–1. The chemicostat controller was not able to react soon enough; the result was an unstable simulation. Unlike the ideal gas simulations when there was no potential energy, $\mu^{*}(t)$ in a dilute gas simulation is not constant. The kinetic energy and potential energy both contribute to $\mu^{*}(t)$,

$$\mu^{*}(t) = \frac{1}{N} \left(\frac{1}{2} \sum_{i=1}^N \sum_{\alpha=1}^3 v_{i,\alpha}^2 + \sum_{i=1}^N \hat{U}_i(\mathbf{r}) \right) \quad 3-35$$

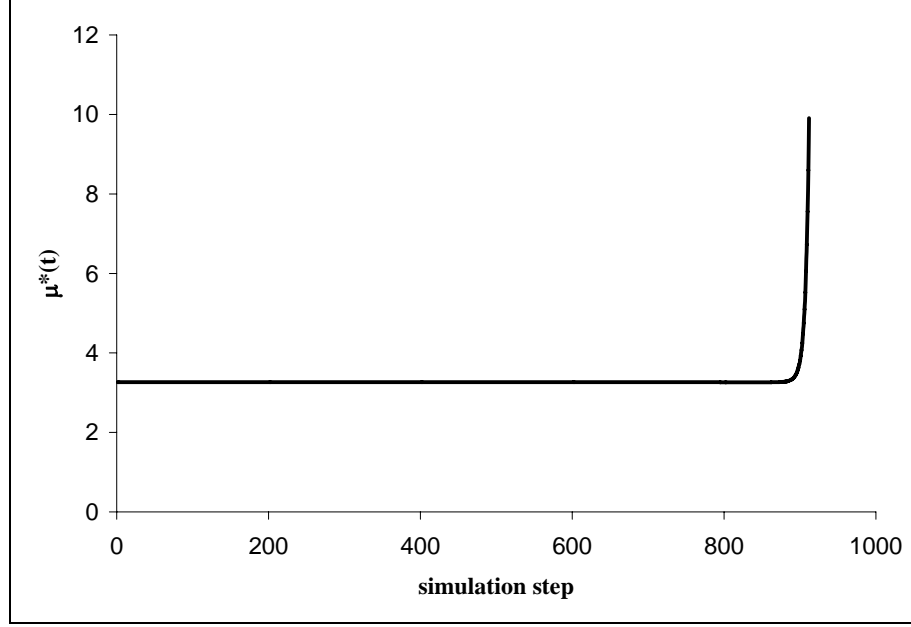


Figure 3.3-1 $\mu^*(t)$ vs. simulation step for a dilute gas system, specific potential energy case, with $\mu^{*set} = \mu^*(t_o)$.

The potential energy contribution to $\mu^*(t)$ is independent of mass. This may cause $\mu^*(t)$ to be unstable. We know that there is a change in potential energy when the number of particles changes in a system; there should also be a change in potential energy when we change the mass of particles. The last term in the partial specific Hamiltonian in equation 3–35 is actually the change in potential energy with respect to the change in mass; this clearly should have a mass dependence in it. In the next section, we test the second formulation of the potential energy as a function of \mathbf{r} and ρ .

3.4 $\mu V \mathcal{E}$ Dilute Gas Simulations Using Potential Energy as a Function of \mathbf{r} and ρ

3.4.1 The Pair Correlation as a Function of \mathbf{r} and ρ

The potential energy expressed as a function of \mathbf{r} and ρ is,

$$U(\mathbf{r}, \rho) = \frac{1}{2} \sum_{i=1}^N \sum_{\substack{j=1 \\ j \neq i}}^N u(r_{ij}(t)) \frac{g(r_{ij}(t), \rho(t)_{effective})}{g(r_{ij}(t), \rho)}$$

3-36

In every simulation step, particle mass changes as well as the effective number density. After evaluating the effective number density, we find the pair correlation function at this effective number density and at the specified simulation density.

There are a number of methods to find the pair correlation function for a given density of a classical monatomic or simple fluid system. We can acquire data from simulation or we can numerically solve an integral equation for the pair correlation. One such expression is from the combination of two equations, the Ornstein Zernike (OZ) Equation and Percus-Yevick (PY) Approximation.

The OZ equation is an equation that defines the direct correlation function, $c(r)$. The direct correlation function is the part of $g(r)$ that involves only the correlations of a central particle and its immediate neighbors. We define an additional function,

$$h(r) \equiv g(r) - 1 \quad 3-37$$

such that the OZ equation is

$$h(r_{12}) \equiv c(r_{12}) + \rho \int_0^\infty c(r_{13}) h(r_{23}) d\mathbf{r}_3 \quad 3-38$$

Basically, the OZ equation is exact because it transfers all of our lack of knowledge of $g(r)$ into another variable, $c(r)$. In other words, we have one equation (the OZ equation) but we have two unknowns, $g(r)$ and $c(r)$. The OZ equation requires a second equation, usually an approximate equation, to be solved. One of the simplest approximations used to “close” the OZ equation is the PY Approximation.

Before we write the PY equation, we first introduce some new variables. First, we define a new variable, the potential of mean force, $w(r)$, as

$$g(r) \equiv \exp[-\beta w(r)] \quad 3-39$$

This is exact because it is simply a definition of $w(r)$. The potential of mean force is the “effective” potential required to generate a given pair correlation function. It cannot be thought of as a pair-wise potential. In the limit that the density goes to zero, the potential of mean force approaches the pair potential. The PY equation approximates the direct correlation function as the difference between a total pair correlation function, $g(r)$, and

an indirect pair correlation function, $y(r)$. This indirect pair correlation function is defined as

$$y(r) \equiv \exp\{-\beta[w(r) - u(r)]\} \quad 3-40$$

The PY approximation is thus

$$c(r) \approx g(r) - y(r) = f(r)y(r) \quad 3-41$$

where $f(r)$ is the force due to the potential of mean force, defined as

$$f(r) \equiv -\frac{\partial}{\partial r} w(r) = \frac{1}{\beta} \frac{\partial}{\partial r} \ln[g(r)] = \frac{1}{\beta g(r)} \frac{\partial g(r)}{\partial r} \quad 3-42$$

The PY equation, (equation 3–41), introduces an approximation for $c(r)$, so that we now have only one equation, the OZ equation, and only one unknown, $g(r)$. [14]

Solving for $g(r)$, we implement an existing code that uses Gillan's Integration Method to solve the OZ-PY [15] that uses the Lennard-Jones interaction potential. We created a database of $g(r)$ at different densities. As we solved for an effective density in the simulation, we searched and interpolated within our database of $g(r_{ij}(t), \rho(t)_{\text{effective}})$.

3.4.2 Simulation Results and Discussions

Chemicostat Controller

First we want to determine if we can run a stable simulation when we have potential energy as a function of distance between particles and density. We summarize the observed behavior of $\mu^*(t)$ from previous simulations: in the ideal gas simulation $\mu^*(t)$ was a constant (Section 3.1); and, in the dilute gas specific potential energy simulation, $\mu^*(t)$ was unstable (Section 3.3). In this dilute gas $U(\mathbf{r}, \rho)$ simulation, we first simulate $\mu^{*set} = \mu^*(t_o)$. In Figure 3.4–1, we show $\mu^*(t)$ is stable, fluctuating about a nearly constant value.

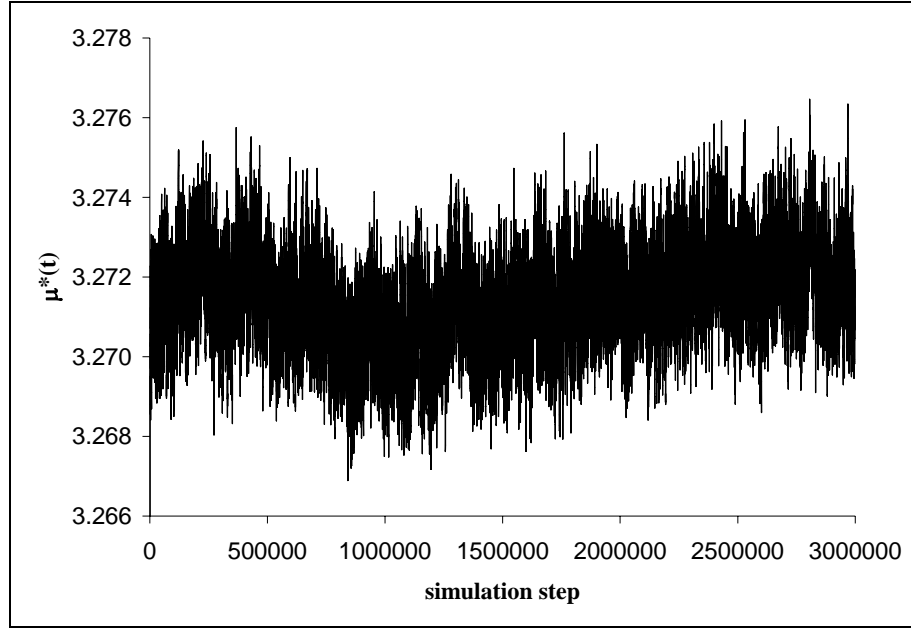


Figure 3.4-1 $\mu^*(t)$ vs. simulation step, from the simulation of a dilute gas system, $U(r,\rho)$ case, with $\mu^{*set} = \mu^*(t_0)$.

With a stable $\mu^*(t)$, we expect that the chemicostat controller can drive the system toward $\mu^{*set} m'$. In Figure 3.4-2, $\mu^*(t)m$ fluctuates about 3.2629, close to the set point of 3.2628. We varied the set point $\mu^{*set} m'$ in different simulations while keeping the system density constant. The average $\mu^*(t)m$ from different simulations are recorded in Table 3.4-1. The simulation average values for $\mu^*(t)m$ are near $\mu^{*set} m'$, indicating that the chemicostat controller is functioning properly.

Now we would like to know if the controller will produce reasonable results if we run simulations at higher densities. While we varied the density, we kept μ^{*set} at 3.262. In Table 3.4-2, we show that we still get average values for $\mu^*(t)m$ close to $\mu^{*set} m'$; the chemicostat controller functions properly at different densities.

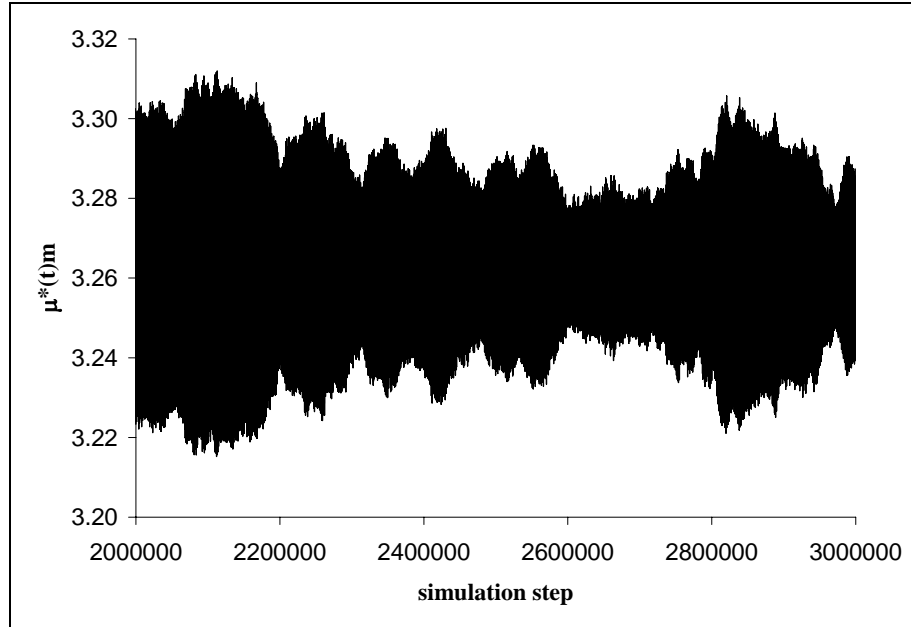


Figure 3.4-2 $\mu^*(t)m$ vs. simulation step from the simulation of a dilute gas system, $U(r,\rho)$ case, with $\mu^{*set} = \mu^*(t_0)$.

Table 3.4-1 Results for Simulations at Different Values of μ^{*set}

$m' \mu^{*set}$	Average $\langle m\mu^*(t) \rangle$	Standard deviation $\langle m\mu^*(t) \rangle$
3.5000	3.5001	0.0206
3.2628	3.2629	0.0215
3.2620	3.2621	0.0192
3.2618	3.2619	0.0199
3.2600	3.2608	0.0435

Table 3.4-2 Results for Simulations at Different Densities

density	Average $\langle m\mu^*(t) \rangle$	Standard Deviation $\langle m\mu^*(t) \rangle$
1.446E-3	3.2621	0.0192
2.100E-3	3.2624	0.0318
3.400E-3	3.2625	0.0372
4.000E-3	3.2622	0.0232
6.000E-3	3.2623	0.0269
8.000E-3	3.2627	0.0406
1.446E-2	3.2624	0.0308

We have said that dilating mass should correspond to changing the number of particles in the system. As properties are sampled in a MD simulation, the most probable value for a property corresponds to the calculated average value of this property. We expect mass to behave as a property controlled in a MD simulation, just like the temperature in a thermostat MD simulation. We show in Figure 3.4–3 that the mass distribution from one of our simulations resembles a Gaussian distribution, and that the mass that occurred the most number of times in the course of the simulation corresponds to the average mass calculated in the simulation. We plot the pair correlation function from one of our simulations in Figure 3.4–4, and we show that the simulation has produced a reasonable particle distribution for a dilute gas system, even as mass changes in our simulation.

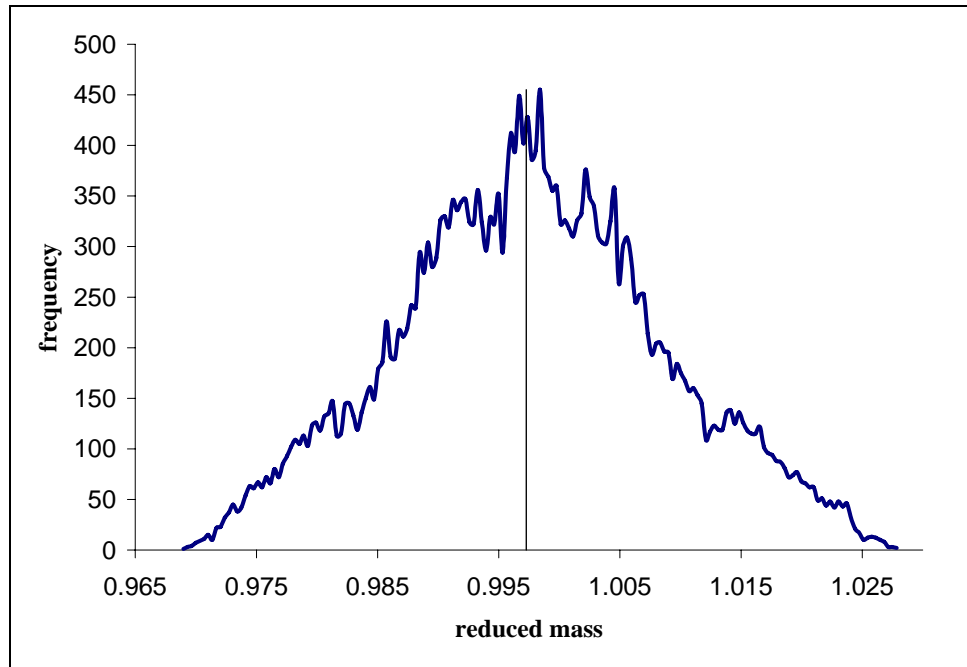


Figure 3.4-3 Mass histogram from the simulation of a dilute gas system, $U(r,\rho)$ case, with $\mu^{*set} = \mu^*(t_0)$.

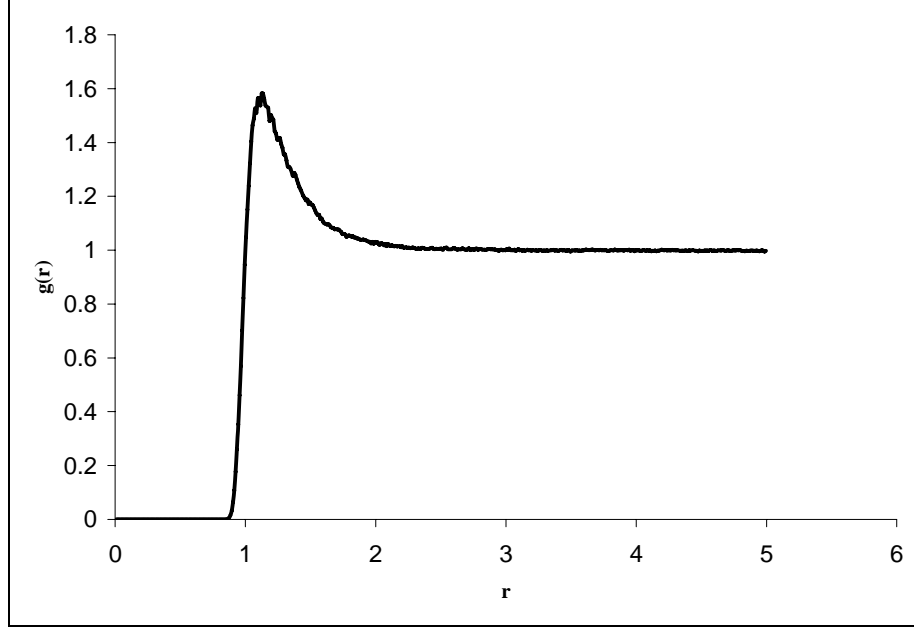


Figure 3.4-4 Pair correlation function from the simulation of a dilute gas system, $U(r,\rho)$ case, with $\mu^{*set} = \mu^*(t_0)$.

The Test for a $\mu V\mathcal{E}$ System

At this point, we need to analyze simulation results to determine whether we are simulating in the $\mu V\mathcal{E}$ ensemble. Specifically, we wanted to compare the partial specific Hamiltonian and the chemical potential. The proper way to compare these two properties is through the change in potential energy, the second term in both equations shown below. Equation 3-43 is the equation for the partial specific Hamiltonian:

$$\mu^*(t) = \frac{1}{N} \left(\frac{1}{2} \sum_{\alpha=1}^3 \sum_{i=1}^N v_{i,\alpha}^2 + \sum_{i=1}^N \frac{\partial U_i(r,\rho)}{\partial m} \right)$$

3-43

The second term on the RHS of equation 3-43 is the change in potential energy with respect to a change in mass. The partial specific Hamiltonian is evaluated at every time step and we record average values of it during a $\mu V\mathcal{E}$ simulation. Equation 3-44 is a statistical mechanical expression for the chemical potential:

$$\mu = -k_B T \ln \left(\frac{V / \Lambda^d}{N+1} \right) - k_B T \ln \int dr_{N+1} \langle \exp(-\beta \Delta U) \rangle_N$$

3-44

The second term on the RHS of equation 3-44 is essentially the average value for the change in potential energy with respect to a change in number of particles in the system. Equation 3-44 is the expression used in Widom's particle insertion method to calculate for the chemical potential of a system. We perform Widom's particle insertion method as we run a NVE simulation to estimate the chemical potential of the system.

Previously, we stated that a change in mass should have the same effect as a change in the number of particles. If we have a box of fixed volume with a number of particles, we know that adding another particle will slightly increase the potential energy inside the box. We relate this increase in number of particles to an increase in mass by considering the equations

$$m = m' \eta_\mu$$

3-45

$$N' = N \eta_\mu$$

3-46

Equation 3-45 is our transformation equation for the mass of the particle. If the mass dilation variable η_μ increases, the mass in the physical (unprimed) frame increases. This increase in mass in the physical frame corresponds to an increase in the number of particles in the aphysical (primed) frame of reference, as shown in equation 3-46. So for our box of fixed volume, adding another particle is equivalent to an increase in mass. An increase in mass should also bring an increase in potential energy.

We compare simulation data for both the change in potential energy with respect to a change in mass and the change in potential energy with respect to a change in the number of particles by converting these to a change in potential energy with respect to a change in system density:

$$\frac{\partial U}{\partial \rho_{\text{widom}}} = V \frac{\partial U}{\partial N}$$

3-47

$$\frac{\partial U}{\partial \rho_{mass}} = m' \frac{V}{N} \frac{\partial U}{\partial m} = m' \frac{V}{N} \frac{\partial U}{m' \partial \eta_\mu} = V \frac{\partial U}{\partial N'}$$

3-48

We distinguish $\partial \mathbf{N}$ from ∂N and from $\partial N'$. The first one is a change in the number of particles from actually changing the number of particles in the system and not mass dilation. The second is the change in the number of particles in the physical frame of reference, and this is zero since N is a constant. The third is the change in number of particles in the primed or aphysical frame of reference; it is equivalent to the expression $N \partial \eta_\mu$.

We can also compare $\frac{\partial U}{\partial \rho_{widom}}$ and $\frac{\partial U}{\partial \rho_{mass}}$ with tabulated values of the average potential energy from $\mu V\mathcal{E}$ and NVE simulations.

In the $\mu V\mathcal{E}$ simulations where $\mu^{*set} m'$ was varied while the system density was kept at a constant, the mass of a particle m was allowed to dilate to drive $\mu^*(t)m$ towards $\mu^{*set} m'$. From these simulations we obtain average values for the dilated mass m and with equations 3-45 and 3-46 the corresponding number of particles in the primed or aphysical frame of reference N' are calculated. Also, with equation 3-9 we calculate the effective density, $\rho(t)_{effective}$ that corresponds to the average dilated mass. From these

$\mu V\mathcal{E}$ simulations we collect $U_{\mu V\mathcal{E}}$ vs. $\rho(t)_{effective}$ data. We can also estimate $\frac{\partial U}{\partial \rho_{U \text{ from } \mu V\mathcal{E}}}$ using centered finite differences on our $U_{\mu V\mathcal{E}} (\rho(t)_{effective})$ data.

We ran NVE simulations at the different effective density values ($\rho(t)_{effective}$) obtained from the $\mu V\mathcal{E}$ simulations. Compared to the $\mu V\mathcal{E}$ simulations, each NVE simulation was at a different set density. These NVE simulations gave average potential energy vs. density data from which we can also estimate $\frac{\partial U}{\partial \rho_{U \text{ from NVE}}}$ using centered finite differences on our $U_{NVE} (\rho(t)_{effective})$ data. We also solved for the potential energy

using the expression for the potential energy as a function of the pair correlation function $g(r)$,

$$\bar{U} = \frac{1}{2} \frac{N^2}{V} \int_0^\infty u(r) g(r) 4\pi r^2 dr$$

3-49

The OZPY approximation was used to solve $g(r)$. Then we used centered finite differences to estimate $\frac{\partial U}{\partial \rho}_{U \text{ from OZPY}}$.

In Figure 3.4–5 we plot the potential energy (U) from μVE simulations, the U from NVE simulations, and the U from integrating the OZPY vs. density. In this U vs. density plot we show that the average U values from μVE simulations are comparable to the average U obtained at NVE simulations and OZPY calculations. The potential energy values from μVE , NVE and OZPY in Figure 3.4–5 follow the same trend with respect to a change in density; therefore, the change in potential energy due to mass dilation

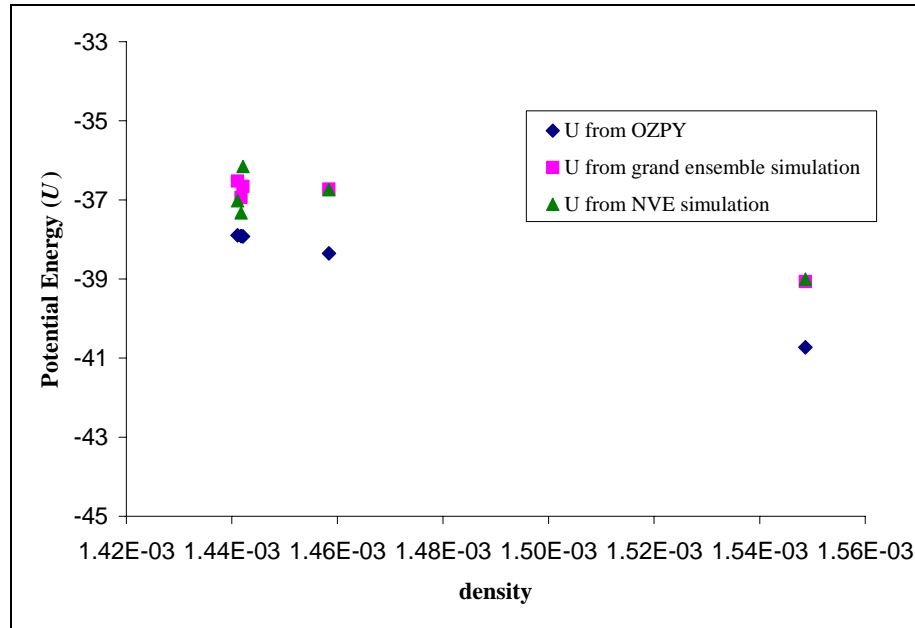


Figure 3.4-5 The potential energy from μVE , NVE and OZPY vs. density.

$\left(\frac{\partial U}{\partial \rho}_{U \text{ from } \mu VE} \right)$ is equivalent to the change in potential energy from change in number of particles in the system $\left(\frac{\partial U}{\partial \rho}_{U \text{ from NVE}} \text{ or } \frac{\partial U}{\partial \rho}_{U \text{ from OZPY}} \right)$.

In Figure 3.4–6 we plot $\frac{\partial U}{\partial \rho}$ from Widom's particle insertion $\frac{\partial U}{\partial \rho}_{widom}$, the change in potential energy with respect to the change in mass $\frac{\partial U}{\partial \rho}_{mass}$, average potential energy from simulation data $\frac{\partial U}{\partial \rho}_{U \text{ from } \mu VE}$ and $\frac{\partial U}{\partial \rho}_{U \text{ from NVE}}$, and calculated potential energy $\frac{\partial U}{\partial \rho}_{U \text{ from OZPY}}$.

The average values $\frac{\partial U}{\partial \rho}_{widom} = -15772$, $\frac{\partial U}{\partial \rho}_{U \text{ from NVE}} = -23874$ and $\frac{\partial U}{\partial \rho}_{U \text{ from OZPY}} = -26291$ all represent the change in potential energy due to change in the number of particles in the system. The $\frac{\partial U}{\partial \rho}_{U \text{ from } \mu VE} = -24949$ represents the change in potential energy due to a change in particle mass. These four values are negative and discrepancy between $\frac{\partial U}{\partial \rho}_{widom}$ and $\frac{\partial U}{\partial \rho}_{U \text{ from NVE}}$, $\frac{\partial U}{\partial \rho}_{U \text{ from } \mu VE}$ and $\frac{\partial U}{\partial \rho}_{U \text{ from OZPY}}$ is possibly due to the difference in the method of averaging the potential energy from Widom's particle insertion. The average of $\frac{\partial U}{\partial \rho}_{mass}$ is 0.007 a very small positive value and a linearly increasing trend. This value was obtained from $\frac{\partial U}{\partial m}$ and it represents the deviation of U as the system goes further from ideal conditions (system effective density increases).

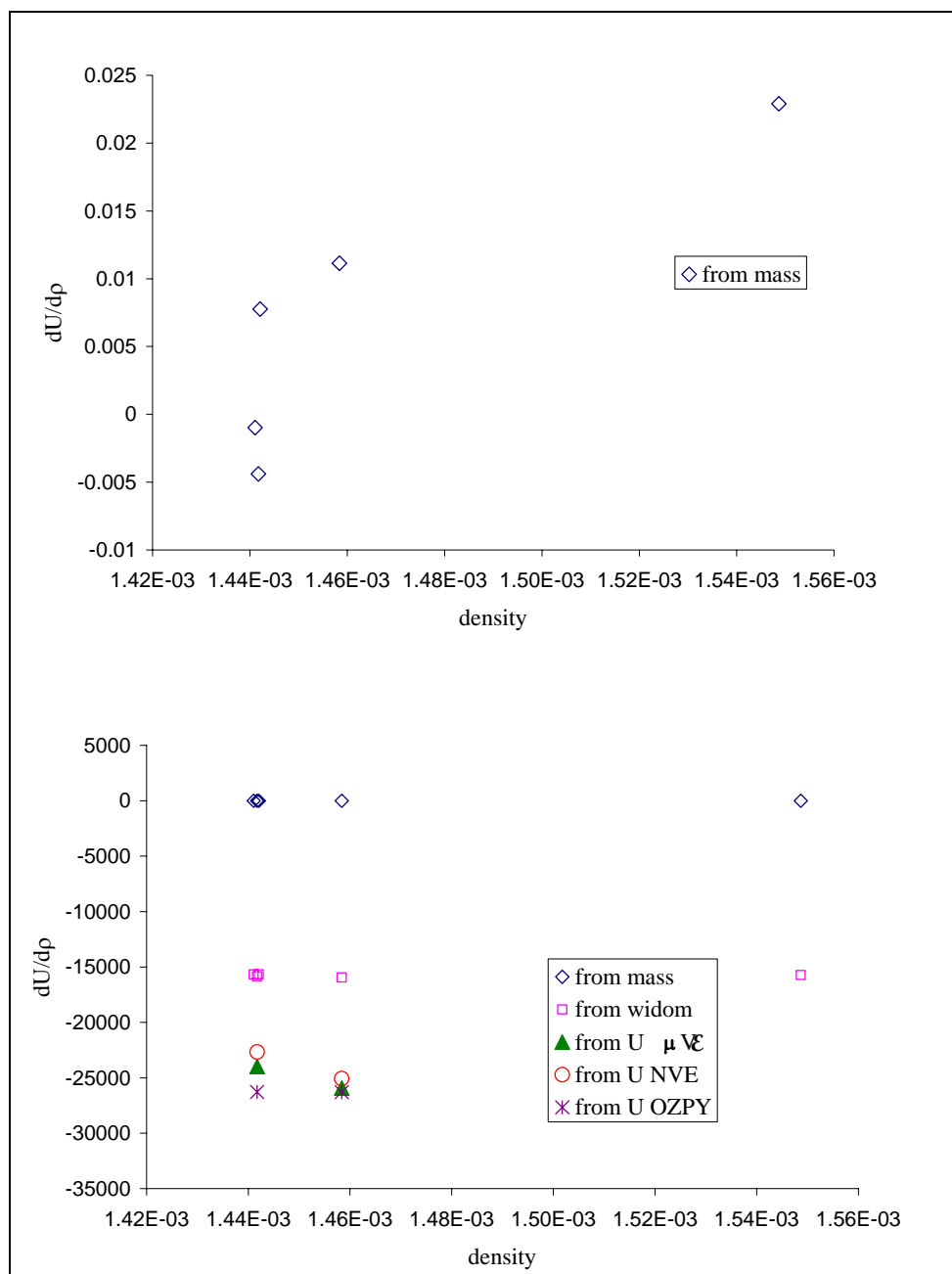


Figure 3.4-6 The change in potential energy with respect to a change in system density vs. density.

We have shown in our simulation data and calculations that the change in mass and the change in number of particles give the same effect on the change in potential energy. As the mass increase, the effective density increase and the potential energy increase in magnitude. From this result we conclude we obtain reasonable simulation results from the $\mu\text{V}\mathcal{E}$ algorithm.

4 Conclusions and Future Work

The primary goal of this work was to create a Hamiltonian-based equilibrium molecular dynamics algorithm for constant chemical potential simulations that does away with particle insertion and deletion. This thesis investigates the possibility of dilating mass instead of changing the number of particles in a $\mu V E$ EMD simulation.

Following the procedure by Keffer *et al.* [1], algorithm development began with formulating a $\mu V E$ Hamiltonian in the primed (aphysical) reference frame where a mass dilation variable was introduced. The equations of motion were derived from this Hamiltonian. One of the equations of motion has a chemicostat controller which controls the partial specific Hamiltonian. Currently there is no known method for evaluating the chemical potential in terms of molecular level properties. Thus, the partial specific Hamiltonian which can be calculated from the molecular level properties such as velocity and potential energy was formulated. The partial specific Hamiltonian is a property similar but not equal to the chemical potential.

The $\mu V E$ EMD algorithm was tested on two systems: an ideal gas and a dilute gas. We test the algorithm whether it is able to control the partial specific Hamiltonian and whether a grand ensemble is simulated.

In both ideal gas and dilute gas simulations, the chemicostat controller functioned properly; it drove the product $m\mu^*(t)$ towards the set point $m'\mu^{*set}$. In the case of the dilute gas simulations, the potential energy expressed as a function of density and the distance between particles resulted in stable simulations that allowed us to test the algorithm further. Specifically, we wanted to determine whether we are performing a $\mu V E$ simulation.

We sought to determine whether our proposed algorithm of increasing mass corresponds to an increase in the number of particles. We know that an increase in particles in a fixed volume should result in an increase in potential energy. We found that a change in mass in simulation is equivalent to a change in number of particles in terms of the effect on the potential energy.

The next step for future work is to use Keffer *et al.*'s [1] methodical procedure for algorithm development and extend the $\mu\mathcal{V}\mathcal{E}$ algorithm to a grand canonical ensemble algorithm.

REFERENCES

1. Keffer, D.J., C. Baig, B.J. Edwards, and P. Adhangale. *A Hamiltonian-Based Algorithm for Rigorous Molecular Dynamics Simulation in the NVE, NVT, NpT, and NpH Ensembles*. in *AIChE Annual Meeting*. 2005. Cincinnati, OH.
2. Hunenberger, P., *Thermostat algorithms for molecular dynamics simulations*, in *Advanced Computer Simulation Approaches For Soft Matter Sciences I*. 2005. p. 105-147.
3. Nosé, S., *A molecular dynamics method for simulations in the canonical ensemble*. Mol. Phys., 1984. **52**(2): p. 255-268.
4. Hoover, W.G., *Canonical Dynamics - Equilibrium Phase-Space Distributions*. Physical Review A, 1985. **31**(3): p. 1695-1697.
5. Keffer, D.J., C. Baig, P. Adhangale, and B.J. Edwards, *A Generalized Hamiltonian-Based Algorithm for Rigorous Equilibrium Molecular Dynamics Simulation in the Canonical Ensemble*. Computer Methods in Applied Mechanics and Engineering, 2005. **submitted**.
6. Nose, S., *A Unified Formulation Of The Constant Temperature Molecular-Dynamics Methods*. Journal Of Chemical Physics, 1984. **81**(1): p. 511-519.
7. Keffer, D.J., C. Baig, P. Adhangale, and B.J. Edwards, *A Generalized Hamiltonian-Based Algorithm for Rigorous Equilibrium Molecular Dynamics Simulation in the Isobaric-Isothermal Ensemble*. Mol. Sim., 2006. **accepted**.
8. Heffelfinger, G.S. and F. Vanswol, *Diffusion In Lennard-Jones Fluids Using Dual Control-Volume Grand-Canonical Molecular-Dynamics Simulation (Dcv-Gcmd)*. Journal Of Chemical Physics, 1994. **100**(10): p. 7548-7552.
9. Cagin, T. and B.M. Pettitt, *Molecular-Dynamics With A Variable Number Of Molecules*. Molecular Physics, 1991. **72**(1): p. 169-175.
10. Papadopoulou, A., E.D. Becker, M. Lupkowski, and F. Vanswol, *Molecular-Dynamics And Monte-Carlo Simulations In The Grand Canonical Ensemble - Local Versus Global Control*. Journal Of Chemical Physics, 1993. **98**(6): p. 4897-4908.
11. Münster, A., *Statistical Thermodynamics*. Vol. 1. 1969, New York: Academic Press.

12. Nosé, S., *A Unified Formulation of the Constant Temperature Molecular-Dynamics Methods*. J. Chem. Phys., 1984. **81**: p. 511-519.
13. Tuckerman, M., B.J. Berne, and G.J. Martyna, *Reversible Multiple Time Scale Molecular-Dynamics*. J. Chem. Phys., 1992. **97**: p. 1990-2001.
14. McQuarrie, D.A., *Statistical Mechanics*. Harper's Chemistry Series, ed. S.A. Rice. 1976, New York: Harper & Row.
15. Lee, L.L., *Molecular thermodynamics of nonideal fluids*. Butterworths series in chemical engineering. 1988, Boston: Butterworths. ix, 497.
16. Mehta, M. and D.A. Kofke, *Molecular Simulation In A Pseudo Grand-Canonical Ensemble*. Molecular Physics, 1995. **86**(1): p. 139-147.

APPENDICES

APPENDIX A

First Version for the Chemicostat Controller

We had begun with a chemicostat controller of the form,

$$\frac{d\zeta_{\mu,\kappa}}{dt} = f_1(\eta_{\mu,\kappa}, v_{\mu,\kappa}^2)(\mu_{\kappa}(t) - \mu_{set,\kappa}) - f_2(\zeta_{\mu,\kappa})$$

A- 1

The Hamiltonian that would give this form for the chemicostat controller is,

$$\begin{aligned} H'_{\mu V\mathcal{E}} = & \sum_{\kappa=1}^c \sum_{i=1}^{M_{\kappa}} \sum_{j=1}^{N_{i,\kappa}} \sum_{\alpha=1}^3 \frac{\eta_{\mu,\kappa} p'^2_{\alpha,j,i,\kappa}}{2 m'_{j,i,\kappa}} + \sum_{\kappa=1}^c \sum_{i=1}^{M_{\kappa}} \sum_{j=1}^{N_{i,\kappa}} U_{j,i,\kappa} \\ & + \sum_{\kappa=1}^c \frac{1}{2} \frac{p^2_{\eta,\kappa}}{Q_{\eta,\kappa}} - \sum_{\kappa=1}^c \eta_{\mu,\kappa} \mu_{\kappa}^{*set} \sum_{i=1}^{M_{\kappa}} \sum_{j=1}^{N_{i,\kappa}} m'_{j,i,\kappa} \end{aligned}$$

A- 2

For a monatomic simple fluid ideal gas equation A-2 simplifies to,

$$H'_{\mu V\mathcal{E}} = \sum_{i=1}^N \sum_{\alpha=1}^3 \frac{\eta_{\mu,\kappa} p'^2_{\alpha,i}}{2 m'_i} + \frac{1}{2} \frac{p^2_{\eta}}{Q_{\eta}} - \eta_{\mu} \mu^{*set} \sum_{i=1}^N m'_i$$

A- 3

We can also write this Hamiltonian in the physical frame of reference as

$$H_{\mu V\mathcal{E}} = \sum_{i=1}^N \sum_{\alpha=1}^3 \frac{1}{2} \frac{p^2_{\alpha,i}}{m_i} + \frac{1}{2} \zeta_{\mu}^2 Q_{\eta} \eta_{\mu}^2 - \mu^{*set} \sum_{i=1}^N m_i$$

A- 4

The equations of motion are derived canonically from the Hamiltonian in the primed frame of reference (equation A-3). This is followed by a noncanonical transformation of the equations of motion from the primed frame of reference to the physical or unprimed frame of reference. The derivation is similar to the procedure illustrated in Chapter 2. Below are the equations of motion derived from equation A-3:

$$\frac{dr_{\alpha,i}}{dt} = \eta_{\mu} \frac{p_{\alpha,i}}{m_i}$$

A- 5

$$\frac{dp_{\alpha,i}}{dt} = p_{\alpha,i} \zeta_{\mu}$$

A- 6

$$\frac{d\eta_\mu}{dt} = \zeta_\mu \eta_\mu$$

A- 7

$$\frac{d\zeta_\mu}{dt} = \frac{Nm_i}{\eta_\mu^2 Q_\eta} (-\mu^*(t) + \mu^{*set}) - \zeta_\mu^2$$

A- 8

The partial specific Hamiltonian for this ideal gas system only has the kinetic energy term since potential energy is negligible. It is a function of the particle velocities.

$$\mu^*(t) = \sum_{i=1}^N \sum_{\alpha=1}^3 \frac{1}{2N} \frac{p_{\alpha,i}^2}{m_i^2} \quad \text{or} \quad \mu^*(t) = \sum_{i=1}^N \sum_{\alpha=1}^3 \frac{1}{2N} v_{\alpha,i}^2$$

A- 9

If we derive the evolution equation for the velocity we see that the velocity, does not change in time:

$$\begin{aligned} p &= mv \\ \frac{dp}{dt} &= v \frac{dm}{dt} + m \frac{dv}{dt} \\ \frac{dv}{dt} &= \frac{1}{m} \frac{dp}{dt} - \frac{v}{m} \frac{dm}{dt} \\ \frac{dv}{dt} &= \frac{1}{m} p \zeta_\mu - \frac{v}{m} m' \eta_\mu \zeta_\mu \\ \frac{dv}{dt} &= 0 \end{aligned}$$

A- 10

In this case, a $\mu V \mathcal{E}$ ideal gas system, $\mu^*(t)$ will not be driven towards μ_{set}^* since the velocity will never change; consequently, $\mu^*(t)$ will not change.

Based on the above, it was apparent that the chemicostat controller A-1 is flawed. The Hamiltonian was revised such that the chemicostat controller, instead of being proportional to the difference between $\mu^*(t)$ and μ^{*set} , was proportional to the difference between $m\mu^*(t)$ and $m'\mu^{*set}$. The mass term was placed with $\mu^*(t)$ so that the dilated mass, m , would drive $m\mu^*(t)$ towards $m'\mu^{*set}$.

APPENDIX B

Procedure for Grand Canonical Equilibrium Molecular Dynamics

Hamiltonian for Grand Canonical EMD

We begin with the $\mu V\mathcal{E}$ Hamiltonian in primed coordinates in Chapter 2 and add thermostat terms, just like in the Nosé-Hoover NVT Hamiltonian. The Hamiltonian of the multicomponent, polyatomic system in the grand canonical ensemble is

$$H'_{\mu VT} = \sum_{\kappa=1}^c \sum_{i=1}^{M_{\kappa}} \sum_{j=1}^{N_{i,\kappa}} \sum_{\alpha=1}^3 \frac{\eta_{\mu,\kappa}}{2 \cdot s^2} m'_{j,i,\kappa} v'^2_{\alpha,j,i,\kappa} + \sum_{\kappa=1}^c \sum_{i=1}^{M_{\kappa}} \sum_{j=1}^{N_{i,\kappa}} U_{j,i,\kappa} \\ + f k_B T_{set} \ln(s) + \frac{1}{2} \frac{p_s^2}{Q_s} + \sum_{\kappa=1}^c \frac{1}{2} \frac{p_{\eta,\kappa}^2}{Q_{\eta,\kappa}} - \sum_{\kappa=1}^c f(\eta_{\mu,\kappa}) \mu_{\kappa}^{*set} \sum_{i=1}^{M_{\kappa}} \sum_{j=1}^{N_{i,\kappa}} m'_{j,i,\kappa}$$

B-1

where we have primed the variables to indicate that they are defined in a frame of reference before we apply a noncanonical transformation. Aside from the mass dilation variable, we now have the time dilation variable, s , in the Hamiltonian. The Hamiltonian in terms of momenta is,

$$H'_{\mu VT} = \sum_{\kappa=1}^c \sum_{i=1}^{M_{\kappa}} \sum_{j=1}^{N_{i,\kappa}} \sum_{\alpha=1}^3 \frac{\eta_{\mu,\kappa}}{2 \cdot s^2} \frac{p'^2_{\alpha,j,i,\kappa}}{m'_{j,i,\kappa}} + \sum_{\kappa=1}^c \sum_{i=1}^{M_{\kappa}} \sum_{j=1}^{N_{i,\kappa}} U_{j,i,\kappa} \\ + f k_B T_{set} \ln(s) + \frac{1}{2} \frac{p_s^2}{Q_s} + \sum_{\kappa=1}^c \frac{1}{2} \frac{p_{\eta,\kappa}^2}{Q_{\eta,\kappa}} - \sum_{\kappa=1}^c f(\eta_{\mu,\kappa}) \mu_{\kappa}^{*set} \sum_{i=1}^{M_{\kappa}} \sum_{j=1}^{N_{i,\kappa}} m'_{j,i,\kappa}$$

B-2

where $f(\eta_{\mu,\kappa})$ represents a function of $\eta_{\mu,\kappa}$.

At this point, we are considering two possible Hamiltonians. The first form of the Hamiltonian is when $f(\eta_{\mu,\kappa}) = \eta_{\mu,\kappa}$,

$$H'_{\mu VT} = \sum_{\kappa=1}^c \sum_{i=1}^{M_{\kappa}} \sum_{j=1}^{N_{i,\kappa}} \sum_{\alpha=1}^3 \frac{\eta_{\mu,\kappa}}{2 \cdot s^2} \frac{p'^2_{\alpha,j,i,\kappa}}{m'_{j,i,\kappa}} + \sum_{\kappa=1}^c \sum_{i=1}^{M_{\kappa}} \sum_{j=1}^{N_{i,\kappa}} U_{j,i,\kappa} \\ + f k_B T_{set} \ln(s) + \frac{1}{2} \frac{p_s^2}{Q_s} + \sum_{\kappa=1}^c \frac{1}{2} \frac{p_{\eta,\kappa}^2}{Q_{\eta,\kappa}} - \sum_{\kappa=1}^c \eta_{\mu,\kappa} \mu_{\kappa}^{*set} \sum_{i=1}^{M_{\kappa}} \sum_{j=1}^{N_{i,\kappa}} m'_{j,i,\kappa}$$

B-3

Another form of the Hamiltonian is when $f(\eta_{\mu,\kappa}) = 2\ln(\eta_{\mu,\kappa}) + 1$ and when we make m' the dilated mass and m the original undilated mass,

$$H'_{\mu VT} = \sum_{\kappa=1}^c \sum_{i=1}^{M_{\kappa}} \sum_{j=1}^{N_{i,\kappa}} \sum_{\alpha=1}^3 \frac{\eta_{\mu,\kappa}^2}{2 \cdot s^2} \frac{p'^2_{\alpha,j,i,\kappa}}{m_{j,i,\kappa}} + \sum_{\kappa=1}^c \sum_{i=1}^{M_{\kappa}} \sum_{j=1}^{N_{i,\kappa}} U_{j,i,\kappa} \\ + f k_B T_{set} \ln(s) + \frac{1}{2} \frac{p_s^2}{Q_s} + \sum_{\kappa=1}^c \frac{1}{2} \frac{p_{\eta,\kappa}^2}{Q_{\eta,\kappa}} - \sum_{\kappa=1}^c (2\ln(\eta_{\mu,\kappa}) + 1) \mu_{\kappa} *_{set} \sum_{i=1}^{M_{\kappa}} \sum_{j=1}^{N_{i,\kappa}} m_{j,i,\kappa}$$

B- 4

We like these two forms because when applying Nosé's Hamiltonian proof, both reduce to the classical form of the μVT ensemble. The first version will give a chemicostat controller of the form equation 2-3, while the second version will give a chemicostat controller of the form 2-4.

We have not been able to get good simulation results from these two forms. The issue is that the chemicostat and thermostat controller counteract each other. Below are the evolution equations for the chemicostat controller and the thermostat controller, which we will derive.

The chemicostat momentum is

$$\frac{d\zeta_{\mu,\kappa}}{dt} = \frac{v_{\mu,\kappa}^2}{\eta_{\mu,\kappa} f k_B T_{set}} \left(- \sum_{i=1}^{M_{\kappa}} \sum_{j=1}^{N_{i,\kappa}} \sum_{\alpha=1}^3 \frac{\eta_T}{2\eta_{\mu,\kappa}} \frac{p^2_{\alpha,j,i,\kappa}}{m_{j,i,\kappa}} - \sum_{i=1}^{M_{\kappa}} \sum_{j=1}^{N_{i,\kappa}} \eta_T U_{j,i,\kappa} \right. \\ \left. + \frac{\eta_T}{\eta_{\mu,\kappa}} \frac{\partial f(\eta_{\mu,\kappa})}{\partial \eta_{\mu,\kappa}} \mu_{\kappa} *_{set} \sum_{i=1}^{M_{\kappa}} \sum_{j=1}^{N_{i,\kappa}} m_{j,i,\kappa} \right) - \eta_T \zeta_{\mu,\kappa}^2$$

B- 5

This equation simplifies to

$$\frac{d\zeta_{\mu,\kappa}}{dt} = \frac{v_{\mu,\kappa}^2 \eta_T}{\eta_{\mu,\kappa}^2 f k_B T_{set}} \left(- \sum_{i=1}^{M_{\kappa}} \sum_{j=1}^{N_{i,\kappa}} \sum_{\alpha=1}^3 \frac{1}{2} \frac{p^2_{\alpha,j,i,\kappa}}{m_{j,i,\kappa}} - \sum_{i=1}^{M_{\kappa}} \sum_{j=1}^{N_{i,\kappa}} \frac{\eta_{\mu,\kappa} \partial U_{j,i,\kappa}}{\partial \eta_{\mu,\kappa}} \right. \\ \left. + \frac{\partial f(\eta_{\mu,\kappa})}{\partial \eta_{\mu,\kappa}} \mu_{\kappa} *_{set} \sum_{i=1}^{M_{\kappa}} \sum_{j=1}^{N_{i,\kappa}} m_{j,i,\kappa} \right) - \eta_T \zeta_{\mu,\kappa}^2$$

B- 6

For a monatomic simple fluid with N particles, the equation for the chemicostat momentum is,

$$\frac{d\zeta_\mu}{dt} = \frac{v_\mu^2 \eta_T}{\eta_\mu^2 f k_B T_{set}} N m_i \left(- \sum_{i=1}^N \sum_{\alpha=1}^3 \frac{1}{2N} \frac{p_{\alpha,j,i,\kappa}^2}{m_{j,i,\kappa}^2} - \sum_{i=1}^N \frac{1}{N} \frac{\partial U_i}{m_i' \partial \eta_\mu} + \frac{\partial f(\eta_\mu)}{\partial \eta_\mu} \mu^{*set} \right) - \eta_T \zeta_\mu^2$$

B- 7

When we substitute equation B-8, the partial specific Hamiltonian, into equation B-7, the equation simplifies to equation B-9:

$$\mu^*(t) = \sum_{i=1}^N \sum_{\alpha=1}^3 \frac{1}{2N} \frac{p_{\alpha,j,i,\kappa}^2}{m_{j,i,\kappa}^2} + \sum_{i=1}^N \frac{1}{N} \frac{\partial U_i}{m_i' \partial \eta_\mu}$$

B- 8

$$\frac{d\zeta_\mu}{dt} = \frac{v_\mu^2 \eta_T}{\eta_\mu^2 f k_B T_{set}} N m_i \left(- \mu^*(t) + \frac{\partial f(\eta_\mu)}{\partial \eta_\mu} \mu^{*set} \right) - \eta_T \zeta_\mu^2$$

B- 9

The thermostat momentum for a monatomic simple fluid with N particles is

$$\frac{d\zeta_T}{dt} = \frac{v_s^2}{f k_B T_{set}} \left(\sum_{i=1}^N \sum_{\alpha=1}^3 \frac{p_{\alpha,i}^2}{m_i} - f k_B T_{set} \right)$$

B- 10

The instantaneous temperature equation can be substituted into equation B-10:

$$T(t) = \frac{\sum_{i=1}^N \sum_{\alpha=1}^3 \frac{p_{\alpha,i}^2}{m_i}}{f k_B}$$

B- 11

Notice that if initially $\mu^{*set} > \mu^*(t)$, then the chemicostat momentum will have a positive value and the mass will increase. When the mass changes the instantaneous temperature, $T(t)$ will be affected and will change also. This will cause the thermostat controller to react to adjust the velocity. When velocity is adjusted, the instantaneous partial specific Hamiltonian will be affected and will cause the chemicostat controller to act once again, changing the mass. This causes the instability of the algorithm. We leave this for future work. Nevertheless, we give the step-by-step procedure of the derivation of the equations of motion for the general form of the Hamiltonian, equation B-2, in the next

section. In the final section, we demonstrate how Nosé's statistical mechanical proof is followed to prove that the μ VT Hamiltonians B-3 and B-4 reduce to the classical form of the μ VT partition function.

Derivation of the equations of motion

As we have done in Chapter 2, we rely on the symplectic relationship between the Hamiltonian and the equations of motion to derive the following evolution equations in the primed frame of reference:

$$\frac{dr'_{\alpha,j,i,\kappa}}{dt'} = \frac{\partial H'_{\mu VT}}{\partial p'_{\alpha,j,i,\kappa}} = \frac{\eta_{\mu,\kappa}}{s^2} \frac{p'_{\alpha,j,i,\kappa}}{m'_{j,i,\kappa}} \quad \text{B- 12}$$

$$\frac{dp'_{\alpha,j,i,\kappa}}{dt'} = -\frac{\partial H'_{\mu VT}}{\partial r'_{\alpha,j,i,\kappa}} = -\frac{\partial U_{\alpha,j,i,\kappa}}{\partial r'} \quad \text{B- 13}$$

$$\frac{d\eta_{\mu,\kappa}}{dt'} = \frac{\partial H'_{\mu VT}}{\partial p_{\eta,\kappa}} = \frac{p_{\eta,\kappa}}{Q_{\eta,\kappa}} \quad \text{B- 14}$$

$$\begin{aligned} \frac{dp_{\eta,\kappa}}{dt'} = -\frac{\partial H'_{\mu VT}}{\partial \eta_{\eta,\kappa}} = & -\sum_{i=1}^{M_\kappa} \sum_{j=1}^{N_{i,\kappa}} \sum_{\alpha=1}^3 \frac{1}{2 \cdot s^2} \frac{p'^2_{\alpha,j,i,\kappa}}{m'_{j,i,\kappa}} - \\ & \sum_{i=1}^{M_\kappa} \sum_{j=1}^{N_{i,\kappa}} \frac{\partial U_{j,i,\kappa}}{\partial \eta_{\eta,\kappa}} + \frac{\partial f(\eta_{\eta,\kappa})}{\partial \eta_{\eta,\kappa}} \mu_\kappa *_{set} \sum_{i=1}^{M_\kappa} \sum_{j=1}^{N_{i,\kappa}} m'_{j,i,\kappa} \end{aligned} \quad \text{B- 15}$$

$$\frac{ds}{dt'} = \frac{\partial H'_{\mu VT}}{\partial p_s} = \frac{p_s}{Q_s} \quad \text{B- 16}$$

$$\frac{dp_s}{dt'} = -\frac{\partial H'_{\mu VT}}{\partial s} = \sum_{\kappa=1}^c \sum_{i=1}^{M_\kappa} \sum_{j=1}^{N_{i,\kappa}} \sum_{\alpha=1}^3 \frac{\eta_{\mu,\kappa}}{s^3} \frac{p'^2_{\alpha,j,i,\kappa}}{m'_{j,i,\kappa}} - \frac{fk_B T_{set}}{s} \quad \text{B- 17}$$

We define a noncanonical transformation to map these equations of motion from the primed or aphysical frame to the physically meaningful (unprimed) frame. The first step is to transform dt' to dt by the relation given by Nosé $dt = s dt'$:

$$\frac{dr'_{\alpha,j,i,\kappa}}{dt} = \frac{\eta_{\mu,\kappa}}{s} \frac{p'_{\alpha,j,i,\kappa}}{m'_{j,i,\kappa}} \quad \text{B- 18}$$

$$\frac{dp'_{\alpha,j,i,\kappa}}{dt} = -s \frac{\partial U_{\alpha,j,i,\kappa}}{\partial r'} \quad \text{B- 19}$$

$$\frac{d\eta_{\mu,\kappa}}{dt} = \frac{s p_{\eta,\kappa}}{Q_{\eta,\kappa}} \quad \text{B- 20}$$

$$\frac{dp_{\eta,\kappa}}{dt} = -\sum_{i=1}^{M_\kappa} \sum_{j=1}^{N_{i,\kappa}} \sum_{\alpha=1}^3 \frac{1}{2 \cdot s} \frac{p'^2_{\alpha,j,i,\kappa}}{m'_{j,i,\kappa}} - \sum_{i=1}^{M_\kappa} \sum_{j=1}^{N_{i,\kappa}} s \frac{\partial U_{j,i,\kappa}}{\partial \eta_{\mu,\kappa}} + s \mu_\kappa^{*set} \sum_{i=1}^{M_\kappa} \sum_{j=1}^{N_{i,\kappa}} m'_{j,i,\kappa} \quad \text{B- 21}$$

$$\frac{ds}{dt} = \frac{s p_s}{Q_s} \quad \text{B- 22}$$

$$\frac{dp_s}{dt} = \sum_{\kappa=1}^c \sum_{i=1}^{M_\kappa} \sum_{j=1}^{N_{i,\kappa}} \sum_{\alpha=1}^3 \frac{\eta_{\mu,\kappa}}{s^2} \frac{p'^2_{\alpha,j,i,\kappa}}{m'_{j,i,\kappa}} - f k_B T_{set} \quad \text{B- 23}$$

The second step is to take the derivatives of the transformation equations (equations B-24 to B-30),

$$m_{j,i,k} = \eta_{\mu,k} m'_{j,i,k} \quad \text{B- 24}$$

$$p_{\alpha,j,i,k} = \frac{\eta_{\mu,k}}{s} p'_{\alpha,j,i,k} \quad \text{B- 25}$$

$$r_{\alpha,j,i,k} = r'_{\alpha,j,i,k} \quad \text{B- 26}$$

$$\eta_{\mu,\kappa} = \eta_{\mu,\kappa} \quad \text{B- 27}$$

$$\zeta_{\mu,\kappa} = \frac{p_{\eta,\kappa}}{\eta_{\mu,\kappa} Q_{\eta,\kappa}} \quad \text{B- 28}$$

$$\zeta_T = \frac{p_s}{Q_s} \quad \text{B- 29}$$

$$\eta_T = s \quad \text{B- 30}$$

The derivatives are

$$\frac{dm_{j,i,k}}{dt} = \eta_{\mu,k} \frac{dm'_{j,i,k}}{dt} + m'_{j,i,k} \frac{d\eta_{\mu,k}}{dt} \quad \text{B- 31}$$

$$\frac{dp_{\alpha,j,i,k}}{dt} = \frac{\eta_{\mu,k}}{s} \frac{dp'_{\alpha,j,i,k}}{dt} - \frac{\eta_{\mu,k}}{s^2} \frac{p'_{\alpha,j,i,k}}{dt} \frac{ds}{dt} + \frac{p'_{\alpha,j,i,k}}{s} \frac{d\eta_{\mu,k}}{dt} \quad \text{B- 32}$$

$$\frac{dr_{\alpha,j,i,k}}{dt} = \frac{dr'_{\alpha,j,i,k}}{dt} \quad \text{B- 33}$$

$$\frac{d\eta_{\mu,\kappa}}{dt} = \frac{d\eta_{\mu,\kappa}}{dt} \quad \text{B- 34}$$

$$\frac{d\zeta_{\mu,\kappa}}{dt} = \frac{1}{\eta_{\mu,\kappa} Q_{\eta,\kappa}} \frac{dp_{\eta,\kappa}}{dt} - \frac{p_{\eta,\kappa}}{\eta_{\mu,\kappa}^2 Q_{\eta,\kappa}} \frac{d\eta_{\mu,\kappa}}{dt} \quad \text{B- 35}$$

$$\frac{d\zeta_T}{dt} = \frac{1}{Q_s} \frac{dp_s}{dt} \quad \text{B- 36}$$

$$\frac{d\eta_T}{dt} = \frac{ds}{dt} = \frac{s p_s}{Q_s} \quad \text{B- 37}$$

The third step is to substitute equations B-18 to B-23 into equations B-31 to B-37:

$$\frac{dr_{\alpha,j,i,\kappa}}{dt} = \frac{\eta_{\mu,\kappa}}{s} \frac{p'_{\alpha,j,i,\kappa}}{m'_{j,i,\kappa}}$$

B- 38

$$\begin{aligned} \frac{dp_{\alpha,j,i,k}}{dt} &= \frac{\eta_{\mu,k}}{s} \frac{dp'_{\alpha,j,i,k}}{dt} - \frac{\eta_{\mu,k}}{s^2} \frac{p'_{\alpha,j,i,k}}{m'_{j,i,k}} \frac{ds}{dt} + \frac{p'_{\alpha,j,i,k}}{s} \frac{d\eta_{\mu,k}}{dt} \\ &= -\eta_{\mu,\kappa} \frac{\partial U_{\alpha,j,i,\kappa}}{\partial r'} - \frac{\eta_{\mu,k}}{s} \frac{p'_{\alpha,j,i,k}}{m'_{j,i,k}} \left(\frac{p_s}{Q_s} \right) + p'_{\alpha,j,i,k} \left(\frac{p_{\eta,\kappa}}{Q_{\eta,\kappa}} \right) \end{aligned}$$

B- 39

$$\frac{d\eta_{\mu,\kappa}}{dt} = \frac{s p_{\eta,\kappa}}{Q_{\eta,\kappa}}$$

B- 40

$$\begin{aligned} \frac{d\zeta_{\mu,\kappa}}{dt} &= \frac{1}{\eta_{\mu,\kappa} Q_{\eta,\kappa}} \frac{dp_{\eta,\kappa}}{dt} - \frac{p_{\eta,\kappa}}{\eta_{\mu,\kappa}^2 Q_{\eta,\kappa}} \frac{d\eta_{\mu,\kappa}}{dt} \\ &= \frac{1}{\eta_{\mu,\kappa} Q_{\eta,\kappa}} \left(-\sum_{i=1}^{M_\kappa} \sum_{j=1}^{N_{i,\kappa}} \sum_{\alpha=1}^3 \frac{1}{2 \cdot s} \frac{p'^2_{\alpha,j,i,\kappa}}{m'_{j,i,\kappa}} - \sum_{i=1}^{M_\kappa} \sum_{j=1}^{N_{i,\kappa}} s U_{j,i,\kappa} \right. \\ &\quad \left. + s \frac{\partial f(\eta_{\mu,\kappa})}{\partial \eta_{\mu,\kappa}} \mu_{\kappa}^{*set} \sum_{i=1}^{M_\kappa} \sum_{j=1}^{N_{i,\kappa}} m'_{j,i,\kappa} \right) - \frac{s p_{\eta,\kappa}^2}{\eta_{\mu,\kappa}^2 Q_{\eta,\kappa}^2} \end{aligned}$$

B- 41

$$\begin{aligned} \frac{d\zeta_T}{dt} &= \frac{1}{Q_s} \frac{dp_s}{dt} \\ &= \frac{1}{Q_s} \left(\sum_{\kappa=1}^c \sum_{i=1}^{M_\kappa} \sum_{j=1}^{N_{i,\kappa}} \sum_{\alpha=1}^3 \frac{\eta_{\mu,\kappa}}{s^2} \frac{p'^2_{\alpha,j,i,\kappa}}{m'_{j,i,\kappa}} - f k_B T_{set} \right) \end{aligned}$$

B- 42

$$\frac{d\eta_T}{dt} = \frac{s p_s}{Q_s}$$

B- 43

Finally, using the transformation equations on the remaining primed variables, the equations of motion in the unprimed frame are

$$\frac{dr_{\alpha,j,i,\kappa}}{dt} = \eta_{\mu,\kappa} \frac{p_{\alpha,j,i,\kappa}}{m_{j,i,\kappa}}$$

B- 44

$$\frac{dp_{\alpha,j,i,\kappa}}{dt} = -\eta_{\mu,\kappa} \frac{\partial U_{\alpha,j,i,\kappa}}{\partial r} - p_{\alpha,j,i,\kappa} \zeta_T + p_{\alpha,j,i,\kappa} \eta_T \zeta_{\mu,\kappa}$$

B- 45

$$\frac{d\eta_{\mu,\kappa}}{dt} = \eta_T \zeta_{\mu,\kappa} \eta_{\mu,\kappa}$$

B- 46

$$\begin{aligned} \frac{d\zeta_{\mu,\kappa}}{dt} = & \frac{v_{\mu,\kappa}^2}{\eta_{\mu,\kappa} f k_B T_{set}} \left(- \sum_{i=1}^{M_\kappa} \sum_{j=1}^{N_{i,\kappa}} \sum_{\alpha=1}^3 \frac{\eta_T}{2\eta_{\mu,\kappa}} \frac{p_{\alpha,j,i,\kappa}^2}{m_{j,i,\kappa}} - \sum_{i=1}^{M_\kappa} \sum_{j=1}^{N_{i,\kappa}} \eta_T U_{j,i,\kappa} \right. \\ & \left. + \frac{\eta_T}{\eta_{\mu,\kappa}} \frac{\partial f(\eta_{\mu,\kappa})}{\partial \eta_{\mu,\kappa}} \mu_{\kappa}^{*set} \sum_{i=1}^{M_\kappa} \sum_{j=1}^{N_{i,\kappa}} m_{j,i,\kappa} \right) - \eta_T \zeta_{\mu,\kappa}^2 \end{aligned}$$

B- 47

$$\frac{d\zeta_T}{dt} = \frac{v_s^2}{f k_B T_{set}} \left(\sum_{\kappa=1}^c \sum_{i=1}^{M_\kappa} \sum_{j=1}^{N_{i,\kappa}} \sum_{\alpha=1}^3 \frac{p_{\alpha,j,i,\kappa}^2}{m_{j,i,\kappa}} - f k_B T_{set} \right)$$

B- 48

$$\frac{d\eta_T}{dt} = \eta_T \zeta_T$$

B- 49

Statistical Mechanical Proof

Hamiltonian Equation B- 3

We begin with the Hamiltonian expressed in laboratory coordinates in the mathematical frame of reference equation B- 3,

$$\begin{aligned} H'_{\mu VT} = & \sum_{\kappa=1}^c \sum_{i=1}^{M_\kappa} \sum_{j=1}^{N_{i,\kappa}} \sum_{\alpha=1}^3 \frac{\eta_{\mu,\kappa}}{2 \cdot s^2} \frac{p'^2_{\alpha,j,i,\kappa}}{m'_{j,i,\kappa}} + \sum_{\kappa=1}^c \sum_{i=1}^{M_\kappa} \sum_{j=1}^{N_{i,\kappa}} U_{j,i,\kappa} \\ & + f k_B T_{set} \ln(s) + \frac{1}{2} \frac{p_s^2}{Q_s} + \sum_{\kappa=1}^c \frac{1}{2} \frac{p_{\eta,\kappa}^2}{Q_{\eta,\kappa}} - \sum_{\kappa=1}^c \eta_{\mu,\kappa} \mu_{\kappa}^{*set} \sum_{i=1}^{M_\kappa} \sum_{j=1}^{N_{i,\kappa}} m'_{j,i,\kappa} \end{aligned}$$

Next, we develop the μ VT partition function. Below, we make use of the definitions

$$N = \sum_{k=1}^c \sum_{i=1}^{M_k} N_{i,k}$$

B- 50

$$d^N p' = dp'_{1,1,1} dp'_{2,1,1} \dots dp'_{N_{M_c,c}, M_c, c}$$

B- 51

$$d^N r' = dr'_{1,1,1} dr'_{2,1,1} \dots dr'_{N_{M_c,c}, M_c, c}$$

B- 52

$$Z'_{\mu VT} = \frac{1}{N!} \int d^N p' \int d^N r' \int dp_{\eta,1} \dots \int dp_{\eta,c} \int d\eta_{\mu,1} \dots \int d\eta_{\mu,c} \int p_s \int ds \delta[H'_{\mu VT} - E]$$

B- 53

We transform the variables from the mathematical frame of reference to the physical frame of reference using the transformation equations from the previous section. The transformation for the momenta \mathbf{p}'_i is broken into two steps for clarity in succeeding steps. First we apply the time dilation, and then the mass dilation:

$$p''_{j,i,k} = \frac{p'_{j,i,k}}{s}$$

B- 54

$$p_{j,i,k} = \eta_{\mu,k} p''_{j,i,k}$$

B- 55

The transformation is applied to the Hamiltonian and to the differentials:

$$\begin{aligned} H_{\mu VT} = & \sum_{k=1}^c \sum_{i=1}^{M_k} \sum_{j=1}^{N_{i,k}} \sum_{\alpha=1}^3 \frac{1}{2} \frac{p_{\alpha,j,i,k}^2}{m_{j,i,k}} + \sum_{k=1}^c \sum_{i=1}^{M_k} \sum_{j=1}^{N_{i,k}} m_{j,i,k} \hat{U}_{j,i,k}(r) + \sum_{k=1}^c \frac{1}{2} \frac{p_{\mu,k}^2}{Q_{\mu,k}} \\ & + f k_B T_{set} \ln(s) + \frac{1}{2} \frac{p_s^2}{Q_s} - \sum_{k=1}^c \mu_k^{*set} \sum_{i=1}^{M_k} \sum_{j=1}^{N_{i,k}} m_{j,i,k} \end{aligned}$$

B- 56

$$d^N p' = s^{D \cdot N} d^N p''$$

B- 57

$$d^N p'' = \prod_{k=1}^c (\eta_{\mu,k})^{D(\sum_{i=1}^{M_k} N_{i,k})} d^N p$$

B- 58

The transformed partition function is thus

$$Z_{\mu VT} = \frac{1}{N!} \int d^N p \int d^N r \int dp_{\eta,1} \dots \int dp_{\eta,c} \int d\eta_{\mu,1} \dots \int d\eta_{\mu,c} \int p_s \int ds s^{D \cdot N} \delta[H_{\mu VT} - E] \cdot \prod_{k=1}^c (\eta_{\mu,k})^{D(\sum_{i=1}^{M_k} N_{i,k})}$$

B- 59

Next, we integrate the partition function over s . We next use a δ -function property, $\delta[G(s)] = \sum_k \delta(s-s_k) / |dG(s)/ds|$, where s_k are all the roots satisfying $G(s)=0$, letting

$$G(s) = H_{\mu VT} - E$$

B- 60

$$G(s_k) = 0$$

B- 61

$G(s)$ has only one root

$$s_k = e^{-\frac{1}{fk_B T_{set}} \left[\sum_{\kappa=1}^c \sum_{i=1}^{M_\kappa} \sum_{j=1}^{N_{i,\kappa}} \sum_{\alpha=1}^3 \frac{1}{2} \frac{p_{\alpha,j,i,\kappa}^2}{m_{j,i,\kappa}} + \sum_{\kappa=1}^c \sum_{i=1}^{M_\kappa} \sum_{j=1}^{N_{i,\kappa}} U_{j,i,\kappa} + \frac{1}{2} \frac{p_s^2}{Q_s} + \sum_{\kappa=1}^c \frac{1}{2} \frac{p_{\eta,\kappa}^2}{Q_{\eta,\kappa}} - \sum_{\kappa=1}^c \mu_{\kappa}^{*set} \sum_{i=1}^{M_\kappa} \sum_{j=1}^{N_{i,\kappa}} m_{j,i,\kappa} - E \right]}$$

B- 62

so that

$$\left| \frac{dG(s)}{ds} \right| = \frac{fk_B T_{set}}{s}$$

B- 63

and

$$\delta[G(s)] = \frac{\delta(s-s_k)}{\left| \frac{dG(s)}{ds} \right|} = \frac{s \cdot \delta(s-s_k)}{fk_B T_{set}}$$

B- 64

We substitute the last expression into the partition function to obtain

$$Z_{\mu VT} = \frac{1}{N! f k_B T_{set}} \int d^N p \int d^N r \int dp_{\eta,1} \dots \int dp_{\eta,c} \int d\eta_{\mu,1} \dots \int d\eta_{\mu,c} \int p_s \int ds s^{D \cdot N + 1} \cdot \delta(s - s_k) \cdot \prod_{k=1}^c (\eta_{\mu,k})^{D(\sum_{i=1}^{M_k} N_{i,k})}$$

B- 65

We use another δ -function property, $\int f(s) \delta(s - s_k) = f(s_k)$, to perform the integration over s :

$$\begin{aligned} f(s) &= s^{D \cdot N + 1} \\ f(s_k) &= s_k^{D \cdot N + 1} \end{aligned}$$

B- 66

The partition function now becomes

$$Z_{\mu VT} = \frac{1}{N! f k_B T_{set}} \int d^N p \int d^N r \int dp_{\eta,1} \dots \int dp_{\eta,c} \int d\eta_{\mu,1} \dots \int d\eta_{\mu,c} \int p_s s_k^{D \cdot N + 1} \prod_{k=1}^c (\eta_{\mu,k})^{D(\sum_{i=1}^{M_k} N_{i,k})}$$

B- 67

$$\begin{aligned} Z_{\mu VT} &= \frac{1}{N! f k_B T_{set}} \int d^N p \int d^N r \int dp_{\eta,1} \dots \int dp_{\eta,c} \int d\eta_{\mu,1} \dots \int d\eta_{\mu,c} \int p_s \prod_{k=1}^c (\eta_{\mu,k})^{D(\sum_{i=1}^{M_k} N_{i,k})} \times \\ &e^{-\frac{D \cdot N + 1}{f k_B T_{set}} \left[\sum_{\kappa=1}^c \sum_{i=1}^{M_\kappa} \sum_{j=1}^{N_{i,\kappa}} \sum_{\alpha=1}^3 \frac{1}{2} \frac{p_{\alpha,j,i,\kappa}^2}{m_{j,i,\kappa}} + \sum_{\kappa=1}^c \sum_{i=1}^{M_\kappa} \sum_{j=1}^{N_{i,\kappa}} U_{j,i,\kappa} + \frac{1}{2} \frac{p_s^2}{Q_s} + \sum_{\kappa=1}^c \frac{1}{2} \frac{p_{\eta,\kappa}^2}{Q_{\eta,\kappa}} - \sum_{\kappa=1}^c \mu_{\kappa}^{*set} \sum_{i=1}^{M_\kappa} \sum_{j=1}^{N_{i,\kappa}} m_{j,i,\kappa} - E \right]} \end{aligned}$$

B- 68

Next, we integrate over p_s . Set $f = DN + 1$. We apply the solution

$$\int_{-\infty}^{\infty} e^{-ax^2} dx = \sqrt{\frac{\pi}{a}} \text{ from integration tables to arrive at}$$

$$\int_{-\infty}^{\infty} e^{-\frac{1}{k_B T_{set}} \frac{p_s^2}{2Q_s}} dp_s = \sqrt{2\pi Q_s k_B T_{set}}$$

B- 69

After integrating over p_s , the partition function becomes

$$\begin{aligned} Z_{\mu VT} &= \frac{C_1}{N! f k_B T_{set}} \int d^N p \int d^N r \int dp_{\eta,1} \dots \int dp_{\eta,c} \int d\eta_{\mu,1} \dots \int d\eta_{\mu,c} \prod_{k=1}^c (\eta_{\mu,k})^{D(\sum_{i=1}^{M_k} N_{i,k})} \times \\ &e^{-\frac{1}{k_B T_{set}} \left[\sum_{\kappa=1}^c \sum_{i=1}^{M_\kappa} \sum_{j=1}^{N_{i,\kappa}} \sum_{\alpha=1}^3 \frac{1}{2} \frac{p_{\alpha,j,i,\kappa}^2}{m_{j,i,\kappa}} + \sum_{\kappa=1}^c \sum_{i=1}^{M_\kappa} \sum_{j=1}^{N_{i,\kappa}} U_{j,i,\kappa} + \sum_{\kappa=1}^c \frac{1}{2} \frac{p_{\eta,\kappa}^2}{Q_{\eta,\kappa}} - \sum_{\kappa=1}^c \mu_{\kappa}^{*set} \sum_{i=1}^{M_\kappa} \sum_{j=1}^{N_{i,\kappa}} m_{j,i,\kappa} \right]} \end{aligned}$$

B- 70

where C_1 is

$$C_1 = \sqrt{2\pi Q_s k_B T_{set}} e^{\frac{E}{k_B T_{set}}}$$

B- 71

Then, we integrate over $p_{\eta,k}$. Using $\int_{-\infty}^{\infty} e^{-ax^2} dx = \sqrt{\frac{\pi}{a}}$ again,

$$\int_{-\infty}^{\infty} e^{-\frac{1}{k_B T_{set}} \frac{p_{\eta,k}^2}{2Q_{\eta,k}}} dp_{\eta,k} = \sqrt{2\pi Q_{\eta,k} k_B T_{set}}$$

B- 72

After integrating over $p_{\eta,k}$, the partition function becomes

$$Z_{\mu VT} = C_2 \int d^N p \int d^N r \int d\eta_{\mu,1} \dots \int d\eta_{\mu,c} \prod_{k=1}^c (\eta_{\mu,k})^{D(\sum_{i=1}^{M_k} N_{i,k})} \times \\ e^{-\frac{1}{k_B T_{set}} \left[\sum_{\kappa=1}^c \sum_{i=1}^{M_{\kappa}} \sum_{j=1}^{N_{i,\kappa}} \sum_{\alpha=1}^3 \frac{1}{2} \frac{p_{\alpha,j,i,\kappa}^2}{m_{j,i,\kappa}} + \sum_{\kappa=1}^c \sum_{i=1}^{M_{\kappa}} \sum_{j=1}^{N_{i,\kappa}} U_{j,i,\kappa} - \sum_{\kappa=1}^c \mu_{\kappa}^{*set} \sum_{i=1}^{M_{\kappa}} \sum_{j=1}^{N_{i,\kappa}} m_{j,i,\kappa} \right]}$$

B- 73

where C_2 is

$$C_2 = \frac{C_1}{N! f k_B T_{set}} \prod_{k=1}^c \sqrt{2\pi Q_{\eta,k} k_B T_{set}}$$

B- 74

We then integrate over $\eta_{\mu,k}$:

$$\int d\eta_{\mu,1} \dots \int d\eta_{\mu,c} \prod_{k=1}^c (\eta_{\mu,k})^{D(\sum_{i=1}^{M_k} N_{i,k})} = \text{constant}, \prod_{k=1}^c C_{\eta,k}$$

The partition function then becomes

$$Z_{\mu VT} = C_2 \prod_{k=1}^c C_{\eta,k} \int d^N p \int d^N r \\ e^{-\frac{1}{k_B T_{set}} \left[\sum_{\kappa=1}^c \sum_{i=1}^{M_{\kappa}} \sum_{j=1}^{N_{i,\kappa}} \sum_{\alpha=1}^3 \frac{1}{2} \frac{p_{\alpha,j,i,\kappa}^2}{m_{j,i,\kappa}} + \sum_{\kappa=1}^c \sum_{i=1}^{M_{\kappa}} \sum_{j=1}^{N_{i,\kappa}} U_{j,i,\kappa} - \sum_{\kappa=1}^c \mu_{\kappa}^{*set} \sum_{i=1}^{M_{\kappa}} \sum_{j=1}^{N_{i,\kappa}} m_{j,i,\kappa} \right]}$$

B- 75

or

$$Z_{\mu VT} = C_2 \prod_{k=1}^c C_{\eta,k} \int d^N p \int d^N r e^{-\frac{1}{k_B T_{set}} \left[\sum_{k=1}^c \sum_{i=1}^{M_k} \sum_{j=1}^{N_{i,k}} \sum_{\alpha=1}^3 \frac{1}{2} \frac{p_{\alpha,j,i,k}^2}{m_{j,i,k}} + \sum_{k=1}^c \sum_{i=1}^{M_k} \sum_{j=1}^{N_{i,k}} U_{j,i,k} \right]} \times \prod_{k=1}^c e^{-\sum_{k=1}^c \frac{\mu_k^{*set}}{k_B T_{set}} \sum_{i=1}^{M_k} \sum_{j=1}^{N_{i,k}} m_{j,i,k}}$$

B- 76

which is proportional to the classical partition function for the μVT ensemble,

$$Q \prod_{k=1}^c e^{-\frac{\bar{\mu}_k^{set}}{k_B T_{set}}} \text{ where } \bar{\mu}_k^{set} = \sum_{k=1}^c \mu_k^{*set} \sum_{i=1}^{M_k} \sum_{j=1}^{N_{i,k}} m_{j,i,k}$$

Hamiltonian Equation B- 4

We begin with the Hamiltonian expressed in laboratory coordinates in the mathematical frame of reference (equation B-4),

$$H'_{\mu VT} = \sum_{\kappa=1}^c \sum_{i=1}^{M_{\kappa}} \sum_{j=1}^{N_{i,\kappa}} \sum_{\alpha=1}^3 \frac{\eta_{\mu,\kappa}^2}{2 \cdot s^2} \frac{p'^2_{\alpha,j,i,\kappa}}{m_{j,i,\kappa}} + \sum_{\kappa=1}^c \sum_{i=1}^{M_{\kappa}} \sum_{j=1}^{N_{i,\kappa}} U_{j,i,\kappa} + f k_B T_{set} \ln(s) + \frac{1}{2} \frac{p_s^2}{Q_s} + \sum_{\kappa=1}^c \frac{1}{2} \frac{p_{\eta,\kappa}^2}{Q_{\eta,\kappa}} - \sum_{\kappa=1}^c (2 \ln(\eta_{\mu,\kappa}) + 1) \mu_{\kappa}^{*set} \sum_{i=1}^{M_{\kappa}} \sum_{j=1}^{N_{i,\kappa}} m_{j,i,\kappa}$$

Then we develop the μVT partition function. Let

$$N = \sum_{k=1}^c \sum_{i=1}^{M_k} N_{i,k}$$

B- 77

$$d^N p' = dp'_{1,1,1} dp'_{2,1,1} \dots dp'_{N_{M_c,c}, M_c, c}$$

B- 78

$$d^N r' = dr'_{1,1,1} dr'_{2,1,1} \dots dr'_{N_{M_c,c}, M_c, c}$$

B- 79

$$Z'_{\mu VT} = \frac{1}{N!} \int d^N p' \int d^N r' \int dp_{\eta,1} \dots \int dp_{\eta,c} \int d\eta_{\mu,1} \dots \int d\eta_{\mu,c} \int p_s \int ds \delta[H'_{\mu VT} - E]$$

B- 80

Next, we transform the variables from the mathematical frame of reference to the physical frame of reference using the transformation equations from the previous section. The transformation for the momenta \mathbf{p}'_i is broken into two steps for clarity in succeeding steps:

$$p''_{j,i,k} = \frac{p'_{j,i,k}}{s}$$

B- 81

$$p_{j,i,k} = \eta_{\mu,k} p''_{j,i,k}$$

B- 82

The transformation is applied to the Hamiltonian and the required differentials through the relationships

$$\begin{aligned} H_{\mu VT} = & \sum_{k=1}^c \sum_{i=1}^{M_k} \sum_{j=1}^{N_{i,k}} \sum_{\alpha=1}^3 \frac{1}{2} \frac{p_{\alpha,j,i,k}^2}{m_{j,i,k}} + \sum_{\kappa=1}^c \sum_{i=1}^{M_{\kappa}} \sum_{j=1}^{N_{i,\kappa}} U_{j,i,\kappa} + \sum_{k=1}^c \frac{1}{2} \frac{p_{\eta,k}^2}{Q_{\eta,k}} \\ & + f k_B T_{set} \ln(s) + \frac{1}{2} \frac{p_s^2}{Q_s} - \sum_{k=1}^c (2 \ln(\eta_{\mu,\kappa}) + 1) \mu_k^{*set} \sum_{i=1}^{M_k} \sum_{j=1}^{N_{i,k}} m_{j,i,k} \end{aligned}$$

B- 83

$$d^N p' = s^{D \cdot N} d^N p''$$

B- 84

$$d^N p'' = \prod_{k=1}^c (\eta_{\mu,k})^{D(\sum_{i=1}^{M_k} N_{i,k})} d^N p$$

B- 85

The transformed partition function is

$$Z_{\mu VT} = \frac{1}{N!} \int d^N p \int d^N r \int dp_{\eta,1} \dots \int dp_{\eta,c} \int d\eta_{\mu,1} \dots \int d\eta_{\mu,c} \int p_s \int ds s^{D \cdot N} \delta[H_{\mu VT} - E] \prod_{k=1}^c (\eta_{\mu,k})^{D(\sum_{i=1}^{M_k} N_{i,k})}$$

B- 86

Now, we integrate the partition function over s . We first use a δ -function property, $\delta[G(s)] = \sum_k \delta(s-s_k) / |dG(s)/ds|$, where s_k are all the roots satisfying $G(s)=0$, let

$$G(s) = H_{\mu VT} - E$$

B- 87

$$G(s_k) = 0$$

B- 88

$G(s)$ has only one root

$$s_k = e^{-\frac{1}{fk_B T_{set}} \left[\sum_{\kappa=1}^c \sum_{i=1}^{M_\kappa} \sum_{j=1}^{N_{i,\kappa}} \sum_{\alpha=1}^3 \frac{1}{2} \frac{p_{\alpha,j,i,\kappa}^2}{m_{j,i,\kappa}} + \sum_{\kappa=1}^c \sum_{i=1}^{M_\kappa} \sum_{j=1}^{N_{i,\kappa}} U_{j,i,\kappa} + \frac{1}{2} \frac{p_s^2}{Q_s} + \sum_{\kappa=1}^c \frac{1}{2} \frac{p_{\eta,\kappa}^2}{Q_{\eta,\kappa}} - \sum_{\kappa=1}^c (2 \ln(\eta_{\mu,\kappa}) + 1) \mu_{\kappa}^{*set} \sum_{i=1}^{M_\kappa} \sum_{j=1}^{N_{i,\kappa}} m_{j,i,\kappa} - E \right]}$$

B- 89

so that

$$\left| \frac{dG(s)}{ds} \right| = \frac{fk_B T_{set}}{s}$$

B- 90

and

$$\delta[G(s)] = \frac{\delta(s-s_k)}{\left| \frac{dG(s)}{ds} \right|} = \frac{s \cdot \delta(s-s_k)}{fk_B T_{set}}$$

B- 91

We substitute the last expression into the partition function

$$Z_{\mu VT} = \frac{1}{N! fk_B T_{set}} \int d^N p \int d^N r \int dp_{\eta,1} \dots \int dp_{\eta,c} \int d\eta_{\mu,1} \dots \int d\eta_{\mu,c} \int p_s \int ds s^{D \cdot N + 1} \delta(s-s_k) \prod_{k=1}^c (\eta_{\mu,k})^{D(\sum_{i=1}^{M_k} N_{i,k})}$$

B- 92

We use another δ -function property, $\int f(s) \delta(s-s_k) = f(s_k)$, to perform the integration over s

$$f(s) = s^{D \cdot N + 1}$$

$$f(s_k) = s_k^{D \cdot N + 1}$$

B- 93

The partition function now becomes,

$$Z_{\mu VT} = \frac{1}{N! f k_B T_{set}} \int d^N p \int d^N r \int dp_{\eta,1} \dots \int dp_{\eta,c} \int d\eta_{\mu,1} \dots \int d\eta_{\mu,c} \int p_s s_k^{D \cdot N + 1} \prod_{k=1}^c (\eta_{\mu,k})^{D(\sum_{i=1}^{M_k} N_{i,k})}$$

B- 94

$$Z_{\mu VT} = \frac{1}{N! f k_B T_{set}} \int d^N p \int d^N r \int dp_{\eta,1} \dots \int dp_{\eta,c} \int d\eta_{\mu,1} \dots \int d\eta_{\mu,c} \int p_s \prod_{k=1}^c (\eta_{\mu,k})^{D(\sum_{i=1}^{M_k} N_{i,k})} \times$$

$$e^{-\frac{D \cdot N + 1}{f k_B T_{set}} \left[\sum_{\kappa=1}^c \sum_{i=1}^{M_\kappa} \sum_{j=1}^{N_{i,\kappa}} \sum_{\alpha=1}^3 \frac{1}{2} \frac{p_{\alpha,j,i,\kappa}^2}{m_{j,i,\kappa}} + \sum_{\kappa=1}^c \sum_{i=1}^{M_\kappa} \sum_{j=1}^{N_{i,\kappa}} U_{j,i,\kappa} + \frac{1}{2} \frac{p_s^2}{Q_s} + \sum_{\kappa=1}^c \frac{1}{2} \frac{p_{\eta,\kappa}^2}{Q_{\eta,\kappa}} - \sum_{\kappa=1}^c (2 \ln(\eta_{\mu,\kappa}) + 1) \mu_{\kappa}^{*set} \sum_{i=1}^{M_\kappa} \sum_{j=1}^{N_{i,\kappa}} m_{j,i,\kappa} - E \right]}$$

B- 95

Next we integrate over p_s . Set $f = DN + 1$. We apply the solution $\int_{-\infty}^{\infty} e^{-ax^2} dx = \sqrt{\frac{\pi}{a}}$ from

integration tables to arrive at

$$\int_{-\infty}^{\infty} e^{-\frac{1}{k_B T_{set}} \frac{p_s^2}{2Q_s}} dp_s = \sqrt{2\pi Q_s k_B T_{set}}$$

B- 96

After integrating over p_s , the partition function becomes

$$Z_{\mu VT} = \frac{C_1}{N! f k_B T_{set}} \int d^N p \int d^N r \int dp_{\eta,1} \dots \int dp_{\eta,c} \int d\eta_{\mu,1} \dots \int d\eta_{\mu,c} \prod_{k=1}^c (\eta_{\mu,k})^{D(\sum_{i=1}^{M_k} N_{i,k})} \times$$

$$e^{-\frac{1}{k_B T_{set}} \left[\sum_{\kappa=1}^c \sum_{i=1}^{M_\kappa} \sum_{j=1}^{N_{i,\kappa}} \sum_{\alpha=1}^3 \frac{1}{2} \frac{p_{\alpha,j,i,\kappa}^2}{m_{j,i,\kappa}} + \sum_{\kappa=1}^c \sum_{i=1}^{M_\kappa} \sum_{j=1}^{N_{i,\kappa}} U_{j,i,\kappa} + \sum_{\kappa=1}^c \frac{1}{2} \frac{p_{\eta,\kappa}^2}{Q_{\eta,\kappa}} - \sum_{\kappa=1}^c (2 \ln(\eta_{\mu,\kappa}) + 1) \mu_{\kappa}^{*set} \sum_{i=1}^{M_\kappa} \sum_{j=1}^{N_{i,\kappa}} m_{j,i,\kappa} \right]}$$

B- 97

where C_1 is

$$C_1 = \sqrt{2\pi Q_s k_B T_{set}} e^{\frac{E}{k_B T_{set}}}$$

B- 98

Now, we integrate over $p_{\eta,k}$. Using $\int_{-\infty}^{\infty} e^{-ax^2} dx = \sqrt{\frac{\pi}{a}}$ again,

$$\int_{-\infty}^{\infty} e^{-\frac{1}{k_B T_{set}} \frac{p_{\eta,k}^2}{2Q_{\eta,k}}} dp_{\eta,k} = \sqrt{2\pi Q_{\eta,k} k_B T_{set}}$$

B- 99

After integrating over $p_{\eta,k}$, the partition function becomes

$$Z_{\mu VT} = C_2 \int d^N p \int d^N r \int d\eta_{\mu,1} \dots \int d\eta_{\mu,c} \prod_{k=1}^c (\eta_{\mu,k})^{D(\sum_{i=1}^{M_k} N_{i,k})} \times \\ e^{-\frac{1}{k_B T_{set}} \left[\sum_{\kappa=1}^c \sum_{i=1}^{M_{\kappa}} \sum_{j=1}^{N_{i,\kappa}} \sum_{\alpha=1}^3 \frac{1}{2} \frac{p_{\alpha,j,i,\kappa}^2}{m_{j,i,\kappa}} + \sum_{\kappa=1}^c \sum_{i=1}^{M_{\kappa}} \sum_{j=1}^{N_{i,\kappa}} U_{j,i,\kappa} - \sum_{\kappa=1}^c (2\ln(\eta_{\mu,\kappa})+1) \mu_{\kappa}^{*set} \sum_{i=1}^{M_{\kappa}} \sum_{j=1}^{N_{i,\kappa}} m_{j,i,\kappa} \right]}$$

B- 100

where C_2 is

$$C_2 = \frac{C_1}{N! f k_B T_{set}} \prod_{k=1}^c \sqrt{2\pi Q_{\eta,k} k_B T_{set}}$$

B- 101

Lastly, we integrate over $\eta_{\mu,k}$. This is the only part where Hamiltonian B-3 and B-4 differ. The “+1” in $2\ln(\eta_{\mu,k})+1$ was necessary in order for the term

$-\sum_{k=1}^c \mu_k \sum_{i=1}^{set} \sum_{j=1}^{M_k} m_{j,i,k}$ to survive this integration step:

$$\int d\eta_{\mu,1} \dots \int d\eta_{\mu,c} \prod_{k=1}^c (\eta_{\mu,k})^{D(\sum_{i=1}^{M_k} N_{i,k})} e^{-\frac{1}{k_B T_{set}} \left[-\sum_{\kappa=1}^c 2\ln(\eta_{\mu,\kappa}) \mu_{\kappa}^{*set} \sum_{i=1}^{M_{\kappa}} \sum_{j=1}^{N_{i,\kappa}} m_{j,i,\kappa} \right]} \\ = \text{constant}, \prod_{k=1}^c C_{\eta,k}$$

The partition function is thus

$$Z_{\mu VT} = C_2 \prod_{k=1}^c C_{\eta,k} \int d^N p \int d^N r \\ e^{-\frac{1}{k_B T_{set}} \left[\sum_{\kappa=1}^c \sum_{i=1}^{M_{\kappa}} \sum_{j=1}^{N_{i,\kappa}} \sum_{\alpha=1}^3 \frac{1}{2} \frac{p_{\alpha,j,i,\kappa}^2}{m_{j,i,\kappa}} + \sum_{\kappa=1}^c \sum_{i=1}^{M_{\kappa}} \sum_{j=1}^{N_{i,\kappa}} U_{j,i,\kappa} - \sum_{k=1}^c \mu_k^{*set} \sum_{i=1}^{M_k} \sum_{j=1}^{N_{i,k}} m_{j,i,k} \right]}$$

B- 102

The partition function can also be expressed as equation B-103 where the proportionality to the classical partition function of the μ VT ensemble is clear:

$$Z_{\mu VT} = C_2 \prod_{k=1}^c C_{\eta,k} \int d^N p \int d^N r e^{-\frac{1}{k_B T_{set}} \left[\sum_{k=1}^c \sum_{i=1}^{M_k} \sum_{j=1}^{N_{i,k}} \sum_{\alpha=1}^3 \frac{1}{2} \frac{p_{\alpha,j,i,k}^2}{m_{j,i,k}} + \sum_{k=1}^c \sum_{i=1}^{M_k} \sum_{j=1}^{N_{i,k}} U_{j,i,k} \right]} \times \prod_{k=1}^c e^{\sum_{k=1}^c \frac{\mu_k^{set}}{k_B T_{set}} \sum_{i=1}^{M_k} \sum_{j=1}^{N_{i,k}} m_{j,i,k}}$$

B- 103

$$Q \prod_{k=1}^c e^{\frac{\bar{\mu}_k^{set}}{k_B T_{set}}} \text{ where } \bar{\mu}_k^{set} = \sum_{i=1}^c \mu_k^{set} \sum_{i=1}^{M_k} \sum_{j=1}^{N_{i,k}} m_{j,i,k}$$

This proof indicates that the algorithm derived from these Hamiltonians could produce rigorous μ VT simulations.

APPENDIX C

Surfactant and Electric Field Strength Effects on Surface Tensions at Liquid/Liquid/Solid Interfaces

This abstract is from a paper by the same name published in the journal 'Langmuir' in 2006 by Johanna M. Santiago, David J. Keffer, and Robert M. Counce:

Santiago, J.M., Keffer, D.J., Counce, R.M., "Surfactant and Electric Field Strength Effects on Surface Tensions at Liquid/Liquid/Solid Interfaces", *Langmuir* **22**(12) 2006 p. 5358-5365.

Reproduced in part with permission from *Langmuir* **22**(12) 2006 p. 5358-5365. Copyright 2006 American Chemical Society.

Abstract

We performed a series of experiments designed to elucidate the effects of the presence of sodium dodecyl sulfate (SDS) surfactant and applied electrical field on the wetting behavior in a system containing a sessile droplet of phenylmethyl polysiloxane (PMPS) oil on a polished stainless steel surface submersed in aqueous solution. The voltage difference ranged from -3V to +3V, which is at least three orders of magnitude smaller than comparable recent work. We report the measured equilibrium contact angle of the droplet as a function of surfactant concentration and field strength. We then modeled the system. We solved Laplace's equation to obtain the three-dimensional field within our system. We expanded the three surface tensions (oil droplet-aqueous solution (oa), oil droplet-metal surface (os), and aqueous solution-metal surface (as)) in Taylor series with respect to surfactant concentration and local field strength. We use these three surface tensions in Young's equation to obtain the theoretical contact angle of the organic droplet. We demonstrate that the large changes in contact angle due to the simultaneous presence of small concentrations of surfactant and small voltage differences can be accounted for by changes in the oa and as surface tensions.

key words: contact angle, droplet detachment, surface potential, electrowetting, surfactant, SDS, PMPS

VITA

Johanna Santiago was born and raised in Quezon City, Philippines. She graduated from the University of the Philippines – Diliman with a Bachelor of Science degree in Chemical Engineering in 2002. She then worked at First Gas Power Corporation in the Philippines for two years before attending the Chemical Engineering M.S. program at the University of Tennessee, Knoxville in August 2004. She will receive the M.S. degree from the University of Tennessee, Knoxville in August 2006.